Lateral organ boundaries 1 is a disease susceptibility gene for citrus bacterial canker disease

Yang Hu, Junli Zhang, Hongge Jia, Davide Sosso, Ting Li, Wolf B. Frommer, Bing Yang, Frank F. White, Nian Wang, and Jeffrey B. Jones

Published Version Information

Citation: Hu, Y., Zhang, J., Jia, H., Sosso, D., Li, T., Frommer, W. B., … Jones, J. B. (2014). *Lateral organ boundaries 1* is a disease susceptibility gene for citrus bacterial canker disease. Proceedings of the National Academy of Sciences of the United States of America, 111(4), E521-E529.

Digital Object Identifier (DOI): doi:10.1073/pnas.1313271111

Publisher's Link: http://www.pnas.org/content/111/4/E521

Lateral organ boundaries 1 is a disease susceptibility gene for citrus bacterial canker disease

Yang Hu[a], Junli Zhang[b], Hongge Jia[c], Davide Sosso[d], Ting Li[e], Wolf B. Frommer[d], Bing Yang[e], Frank F. White[b], Nian Wang[c], and Jeffrey B. Jones[a,1]

[a]Department of Plant Pathology, University of Florida, Gainesville, FL 32611; [b]Department of Plant Pathology, Kansas State University, Manhattan, KS 66506; [c]Citrus Research and Education Center, University of Florida, Lake Alfred, FL 33850; [d]Department of Plant Biology, Carnegie Institution for Science, Stanford, CA 94306; and [e]Department of Genetics, Development, and Cell Biology, Iowa State University, Ames, IA 50011

Edited by Brian J. Staskawicz, University of California, Berkeley, CA, and approved December 18, 2013 (received for review July 15, 2013)

Citrus bacterial canker (CBC) disease occurs worldwide and incurs considerable costs both from control measures and yield losses. Bacteria that cause CBC require one of six known type III transcription activator-like (TAL) effector genes for the characteristic pustule formation at the site of infection. Here, we show that *Xanthomonas citri* subspecies *citri* strain Xcc306, with the type III TAL effector gene *pthA4* or with the distinct yet biologically equivalent gene *pthAw* from strain XccA^{w}, induces two host genes, *CsLOB1* and *CsSWEET1*, in a TAL effector-dependent manner. *CsLOB1* is a member of the Lateral Organ Boundaries (LOB) gene family of transcription factors, and *CsSWEET1* is a homolog of the SWEET sugar transporter and rice disease susceptibility gene. Both TAL effectors drive expression of *CsLOB1* and *CsSWEET1* promoter reporter gene fusions when coexpressed in citrus or *Nicotiana benthamiana*. Artificially designed TAL effectors directed to sequences in the *CsLOB1* promoter region, but not the *CsSWEET1* promoter, promoted pustule formation and higher bacterial leaf populations. Three additional distinct TAL effector genes, *pthA, *pthB*, and *pthC*, also direct pustule formation and expression of *CsLOB1*. Unlike *pthA4* and *pthAw*, *pthB* and *pthC* do not promote the expression of *CsSWEET1*. *CsLOB1* expression was associated with the expression of genes associated with cell expansion. The results indicate that CBC-inciting species of *Xanthomonas* exploit a single host disease susceptibility gene by altering the expression of an otherwise developmentally regulated gene using any one of a diverse set of TAL effector genes in the pathogen populations.**

Citrus bacterial canker (CBC) is a severe disease with worldwide distribution affecting all of the commercially important citrus species and cultivars. The disease is caused by two species of bacteria in the genus *Xanthomonas*. The most widespread species is *Xanthomonas citri* subspecies (ssp.) *citri* (Xcc) and was originally identified in Asia. The disease is believed to have subsequently spread from Southeast Asia to other citrus growing regions. Strains of Xcc are further distinguished according to their host ranges. Type A strains of Xcc cause disease on most species of citrus, whereas type A^{w} and type A* strains are restricted to Key lime (*Citrus aurantiifolia*) (1–3). A second genetically distinct species, *Xanthomonas fuscans* ssp. *aurantifolii* (Xfa), is grouped into type B and type C. Outbreaks occur sporadically. In Florida, for example, the last extensive outbreak involving type A strains occurred in 1995, triggering an ultimately unsuccessful eradication program that ended in 2006, costing an estimated $1 billion, and stimulated renewed efforts for more effective and economical control methods (4).

Genomic resources exist for citrus species, including draft genome sequences of several species and extensive expression sequence tags (ESTs) of mRNAs from different developmental and disease states (5, 6). A variety of transcription profiling studies of diseased hosts with citrus bacterial canker have been conducted, comparing susceptible and resistant host reactions (7, 8). Genes involved in host defense, cell-wall remodeling, vesicle trafficking, and cell division genes were identified that may be involved in disease development.

Equally good genomic resources are available for the bacterial pathogens. Genome sequences are available for representative strains of Xcc type A, Xcc type A^{w}, Xfa type B, and Xfa type C (9–11). Both Xcc and Xfa contain type III secretion systems (T3SS), although the contributions, biochemically and functionally, of the individual substrate effectors are unknown. Xcc-A and Xcc-A^{w} contain 24 and 30 putative type 3 secretion (T3S) effectors, respectively, whereas Xfa-B and Xfa-C contain 27 and 26 T3S effectors, respectively (10). Loss of T3SS function in Xcc results in complete loss of disease symptoms and reduced bacterial populations in host tissue. However, phenotypic effects have only been observed upon mutation of several individual effector genes (12–14). The host range restriction of type A^{w} strains to Key lime has been attributed to the presence of T3S effector AvrGf1, whereas the characteristic symptom of pustule formation in citrus bacterial canker is dependent on different members of the AvrBs3/PthA family of T3SS effectors, known collectively as transcription activator-like (TAL) effectors (3, 15).

TAL effectors have been shown to direct the induction of specific disease susceptibility (S) and resistance (R) host genes during infection (16). TAL effectors bind to plant DNA elements within the promoter regions via a series of amino acid repeats in the coding central portion (17–19). PthA from Xcc was the first TAL effector to be associated with a distinct virulence function in infections, controlling both pustule formation and the level of bacterial leaf populations (20). Transient expression of *pthA* inside the host cells has been reported to induce CBC-like symptoms in excised leaf tissue (21). One target of the TAL effector AvrBs3

Significance

Citrus bacterial canker, which is caused by several species in the genus *Xanthomonas*, is a severe disease with worldwide distribution affecting all the commercially important citrus species and cultivars. The mechanisms of canker development, involving erumpent pustule formation and bacterial growth, are not known. Our findings suggest that virulence determinants in several pathogens activate a single host disease susceptibility (S) gene that has a critical contribution to bacterial growth and host pustule development. The S gene represents an excellent candidate for control measures for the citrus bacterial canker.

Author contributions: Y.H., J.Z., W.B.F., B.Y., F.F.W., N.W., and J.B.J. designed research; Y.H., J.Z., H.J., D.S., and T.L. performed research; F.F.W. contributed new reagents/analytic tools; Y.H., J.Z., W.B.F., F.F.W., N.W., and J.B.J. analyzed data; and Y.H., J.Z., W.B.F., F.F.W., N.W., and J.B.J. wrote the paper.

The authors declare no conflict of interest.

This article is a PNAS Direct Submission.

Data deposition: Microarray data reported in this paper have been deposited in the Gene Expression Omnibus (GEO) database, www.ncbi.nlm.nih.gov/geo (GEO accession no. GSE50741).

[1]To whom correspondence should be addressed. E-mail: jbjones@ufl.edu.

This article contains supporting information online at www.pnas.org/lookup/suppl/doi:10.1073/pnas.1313271111/-/DCSupplemental.

from *Xanthomonas campestris* pathovar (pv.) *vesicatoria* is *upa20*, which encodes a bHLH family transcriptional factor and acts as a regulator of cell enlargement in *Nicotiana benthamiana* (22). In rice, two major S genes, *Os8N3* (*OsSWEET11*) and *Os11N3* (*OsSWEET14*), are targets of the TAL effectors PthXo1 and AvrXa7, respectively, from the bacterial blight pathogen *X. oryzae* pv. *oryzae*, and strains that depend on either PthXo1 or AvrXa7 for full virulence and cannot induce either *Os8N3* or *Os11N3* due to host mutations or suppression of host gene expression are weakly virulent. *Os8N3* and *Os11N3* products are not related to *upa20*, and both are closely related members of a family of sugar transporters (23–25). Different TAL effectors can induce the same gene in the host. In pepper, *upa20* is also the target of AvrHah1 from *Xanthomonas gardneri* (26, 27). In rice, *Os11N3* is induced by any of three TAL effectors from *Xanthomonas oryzae* pv. *oryzae*, AvrXa7 and PthXo3, or TalC (24, 28). An S gene with minor effects on susceptibility in bacterial blight of rice encodes a bZIP transcription factor and is the target of yet another TAL effector, PthXo6 (29).

Representative strains of the five different types responsible for citrus canker, A, A*, A^w, B, and C, contain at least one *pthA* homolog, which are designated *pthA*, *pthA**, *pthAw*, *pthB*, and *pthC*, respectively, and essential for pustule formation on citrus (30). Although closely related, each gene has a unique repetitive central domain. Xcc strain 306 contains four TAL effector genes, of which *pthA4* is known to be required for pustule formation (12). Hypothetically, TAL effectors of Xcc and Xfa induce one or more host genes that result in pustule formation. Here, we combined transcription profiling of host responses to strains of Xcc that vary in TAL effector gene content, TAL effector binding element (EBE) prediction, and artificial TAL effectors designed to identify S genes of citrus.

Results

Experimental Design. To identify the targets of TAL effectors that are involved in citrus canker, a strategy was devised to identify and test candidate target genes whose expression was dependent on the presence of representative *pth* genes from Xcc (Fig. 1*A*). In brief, near isogenic strains were constructed from a TAL effector mutant strain that was incapable of pustule formation. Expression profiles were then conducted on host tissue after inoculation with either wild-type or complemented strain and compared with the pustule-defective parent strain. Candidate S genes were selected from the common TAL effector-dependent expressed genes based on the fold increase in expression, presence of a candidate EBE in the promoter regions, and relatedness to known S genes. The candidate genes were then subjected to complementation by artificially designed TAL effectors (dTALes) that were either optimized by the consensus TAL effector binding codes or targeted to novel promoter sequences. Optimization and novel EBE targeting allow for resolution of collaterally induced or so-called "off-target" genes and the intended host S genes.

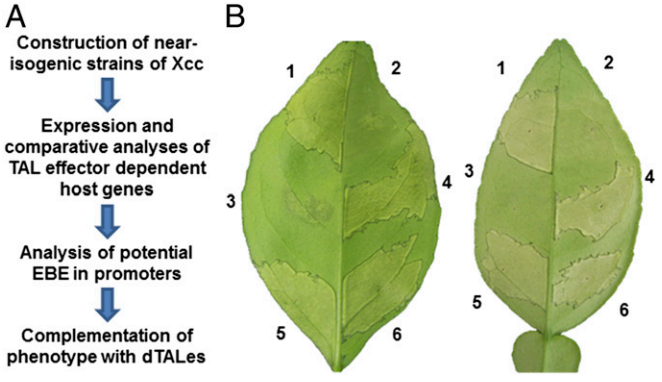

Fig. 1. TAL effectors PthA4 and PthAw are required and sufficient for pustule formation in sweet orange and grapefruit. (*A*) Experimental design scheme for this study. (*B*) Loss of *pthA4* eliminated pustule formation in sweet orange cultivar (cv.) Valencia (*Left*) and grapefruit cv. Duncan (*Right*), which was restored by PthA4 and PthAw. Panels: 1, inoculations with wild-type Xcc306; 2, *pthA4* deletion mutant Xcc306Δ*pthA4*; 3, water (mock) inoculation; 4, triple-deletion mutant Xcc306Δ*pthA1*Δ*pthA2*Δ*pthA3* (with intact *pthA4*); 5, Xcc306Δ*pthA4*::*pthA4*; 6, Xcc306Δ*pthA4*::*pthAw*. The leaves were photographed 5 d after infiltration.

Deletions of each individual TAL effector gene of Xcc306 as well as a triple genes mutant, Xcc306Δ*pthA1pthA2pthA3*, were constructed (Fig. S1*A*). Previous work had shown that the loss of *pthA4* resulted in loss of pustule formation (12). The triple mutant was constructed to determine if *pthA4* alone was sufficient for pustule formation. As previously observed, only the strain with a deletion of *pthA4* (Xcc306Δ*pthA4*) showed loss of pustule formation on sweet orange and grapefruit (Fig. 1*B*). The triple mutant, lacking *pthA1-3* and retaining *pthA4*, showed no change in pustule-forming ability (Fig. 1*B*). Two near-isogenic strains of Xcc306Δ*pthA4* were constructed containing *pthA4* (Xcc306Δ*pthA4*::*pthA4*) or *pthAw* (Xcc306Δ*pthA4*::*pthAw*). Both complemented strains showed symptoms similar to the wild-type Xcc306, indicating that *pthA4* was required and sufficient for pustule formation on sweet orange and grapefruit (Fig. 1*B*).

***CsLOB1* and *CsSWEET1* Are Candidate Targets of TAL Effectors PthA4 and PthAw.** Microarray analyses using the Affymetrix GeneChip Citrus Array were performed on host mRNA following inoculation with the mutant strain Xcc306Δ*pthA4*, the parental strain with *pthA4* (Xcc306) and Xcc306Δ*pthA4*::*pthAw*. Young leaf tissues of sweet orange and grapefruit were infiltrated with Xcc306 (containing *pthA4*), Xcc306Δ*pthA4*::*pthAw*, and Xcc306Δ*pthA4*, and samples were collected at 120 h postinfection. The genes that showed significantly higher (adjusted $P \leq 0.01$) expression levels in tissue infiltrated with wild-type Xcc306 or Xcc306Δ*pthA4*::*pthAw* in comparison with tissue infiltrated with Xcc306Δ*pthA4* were selected as potential candidate host S genes (Table 1). The promoter regions of the most highly up-regulated genes in either sweet orange or grapefruit were scanned for probable PthA4 or PthAw binding elements (*Materials and Methods*). The EBEs were predicted based on the repeat variable diresidues (RVDs) and TAL code (Fig. S2*A*). Two genes, one represented by probe sets Cit.37210.1.S1_at and Cit.35190.1.S1_at and the second by set Cit.3027.1.S1_s_at, had candidate EBEs and were characterized further.

The gene represented by probes Cit.37210.1.S1_at and Cit.35190.1.S1_at contained promoter proximal sequence very close to the canonical PthA4 binding element (EBE_{PthA4}) located 92 bp upstream of predicted transcription start site, which was based on EST sequences from both sweet orange and grapefruit (Table 1; Fig. S2*B*). Another gene, which is represented by Cit.3027.1.S1_s_at, contained two candidate EBEs. The first one starts 43 bp upstream of the predicted transcription start site and coincides with putative TATAA box, which was labeled site A; the second one, site B, was found at 85 bp upstream of the start site and was similar to the canonical PthAw EBE (Table 1; Fig. S2*C*). The expression of both genes was observed to be elevated as determined by quantitative RT-PCR (qRT-PCR) analysis of mRNA from tissue infected either with Xcc306 or Xcc306Δ*pthA4*::*pthAw* in comparison with mRNA from tissue infected with Xcc306Δ*pthA4* in sweet orange (Fig. 2) and in grapefruit (Fig. S3). A time course of 12, 24, and 48 h after inoculation in sweet orange indicated that expression of both genes reached high levels by 24 h after the infiltration (Fig. 2). Cit.37210.1.S1_at and Cit.35190.1.S1_at represent a gene encoding a member of the Lateral Organ Boundaries (LOB) domain family of transcription factors and was designated as *CsLOB1* (Fig. S4*A*). The most closely related homologs in *Arabidopsis* are AtLBD1 and AtLBD11

Table 1. Combined top 10-fold induced genes for PthA4 and PthAw

Affymetrix ID	LFC, *Cs* PthA4	LFC, *Cp* PthAw	DNA	EBE	Annotation
Cit.28626.1.S1_s_at	9.357	—	CV710534	No	β-expansin 6
Cit.9528.1.S1_x_at	8.176	—	CX641267	No	β-expansin 2
Cit.5370.1.S1_s_at	8.088	3.164	CX642883	No	Invertase inhibitor
Cit.20041.1.S1_at	7.587	3.402	CB250345	No	No hit
Cit.37210.1.S1_at	7.164	3.434	BQ623314	Yes	LOB domain
Cit.35754.1.S1_at	6.973	3.296	CB250305	No	Polygalacturonase-like
Cit.7877.1.S1_at	6.728	—	CX667721	No	Expansin B2
Cit.9020.1.S1_s_at	6.42	—	CX305834	No	Lipid binding
Cit.35190.1.S1_at*	6.342	3.450	CK932995	Yes	LOB domain
Cit.2392.1.S1_at	6.305		CF831790	No	Acidic cellulase
Cit.3027.1.S1_s_at	—	4.376	CX048987	Yes	Nodulin MtN3
Cit.15355.1.S1_at	—	3.413	CB291618	No	Oxidoreductase
Cit.18912.1.S1_x_at	—	3.073	CX301535	No	Germin-like
Cit.11963.1.S1_at	—	2.993	CF829030	No	Proline-rich PRP1
Cit.35756.1.S1_at	—	2.935	CB250319	No	Endopolygalacturonase

Cs, sweet orange (*C. sinensis*); *Cp*, grapefruit (*C. paradise*); LFC, $\log_2$ fold-change.
*Represents the same gene as Cit.37210.1.S1_at.

(Fig. S4*B*). Cit.3027.1.S1_s_at represents a homolog to the TAL effectors targeted S genes *OsSWEET11* and *OsSWEET14* in rice, and was designated as *CsSWEET1*. *CsSWEET1* product is most closely related to members of Clade I that includes AtSWEET1 of *Arabidopsis* (Fig. S4*C*). Measurements of sugar transport by CsSWEET1 in the HEK293T cells indicated that the transporter could mediate both glucose and sucrose transport activity (Fig. 3). In the assay, entrance of the sugar into the cell interferes with the fluorescence of the particular sensor—in this case, either FLIPsuc90μΔ1V or FLIPglu600μD13V.

***CsLOB1* and *CsSWEET1* Promoters Direct TAL Effector-Dependent Expression.** The respective promoters of *CsSWEET1* and *CsLOB1* were fused to the *uidA* [β-glucuronidase (GUS)] reporter gene and expressed transiently by *Agrobacterium*-mediated transfer. Truncated and versions with alterations in the predicted EBEs were tested in coinoculation assays with Xcc in citrus leaves (Fig. 4*A*). The wild-type promoter fragment of *CsSWEET1* directed GUS activity when coinoculated with the wild-type strain Xcc306 and the complemented strain Xcc306Δ*pthA4::pthA4*, whereas no GUS activity was observed when coinfiltrated with strain Xcc306Δ*pthA4* (Fig. 4*B*; CsSWPwt). Coinoculations with the truncated, substituted, and deleted versions of *CsSWEET1* promoter and Xcc306 resulted in little or no GUS activity, indicating noncanonical structure to the candidate EBEs of *CsSWEET1* (Fig. 4; CsSWPT, CsSWPM1, and CsSWPD, respectively). Wild-type, truncated, and substituted versions of *CsLOB1* promoter were activated to the same approximate level (Fig. 4; CsLOBPT and CsLOBPM1). The deletion within the predicted EBE and TATAA box of *CsLOB1* (Fig. 4*A*; CsLOBPD) resulted in the loss of PthA4-mediated expression (Fig. 4*B*).

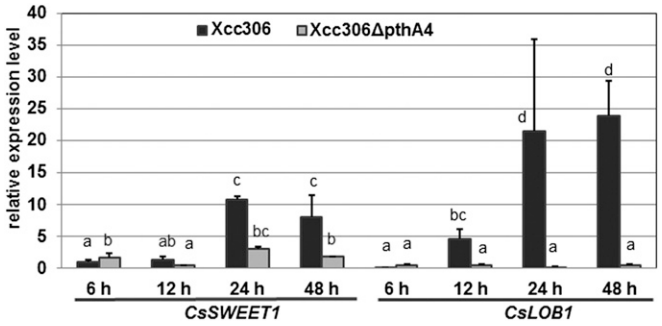

Fig. 2. *CsSWEET1* and *CsLOB1* are induced by PthA4. The expression level of *CsSWEET1* and *CsLOB1* reached peak levels at 24 h postinoculation of Xcc306 on sweet orange. Xcc306Δ*pthA4* did not induce either gene. Total RNA was isolated at 6, 12, 24, and 48 h after inoculation. The expression was normalized to housekeeping gene *EF1α*. Data represent the mean ± SD; different lowercase letters represent significant differences ($P \leq 0.01$) using ANOVA analysis and Tukey test.

The results for the alterations to *CsSWEET1* and *CsLOB1* promoters indicated that, although remarkably similar, the promoters of the respective genes with respect to the candidate EBEs have important differences. Based on the results with the truncated version CsLOBPT, the candidate EBE_{PthA4} for *CsLOB1* is contained within the region of the TATAA box (Fig. 4*A*, construct 8). Additional base substitutions and insertions were created and tested within the truncated version of *CsLOB1* to further corroborate the function of this region as an EBE_{PthA4} (Fig. 4*A*, constructs 8–12). Promoter variant CsLOBPM3, which has a substitution of GG for CC at the eighth and ninth positions in the EBE, had a severe effect on PthA4-dependent promoter activity, whereas the lone substitution of T (CsLOBPM3) at position 8 had little effect on activity. A single nucleotide insertion at position 11 (CsLOBPins) in EBE_{PthA4} resulted in loss of GUS activity (Fig. 4*B*, constructs 9–11). By contrast, the promoter of another highly up-regulated gene, Cit.7877.1.S1_at, was not able to be induced by PthA4 (Fig. 4*B*, construct 13). Placement of the EBE_{PthA4} from *CsLOB1* at 20 bp upstream of putative TATAA box in the Cit. 7877 promoter resulted in PthA4-dependent expression of Cit. 7877.1.S1_at (Fig. 4*B*, construct 14). *Agrobacterium tumefaciens*-mediated transient ectopic expression of *pthA4* or *pthAw* was also able to activate the same *CsLOB1* or *CsSWEET1* promoter patterns in *N. benthamiana*, respectively (Fig. S5).

Artificial dTALes Targeting *CsLOB1* Induce Pustule Formation. Artificial dTALe genes using *pthA4* as a backbone sequence were designed with repeats specifically targeting unique sequences within promoters of *CsSWEET1* and *CsLOB1*, respectively, using optimized repeat variable di-amino acid (RVD) residues (Fig. 5*A*). The genes were designated *dCsLOB1.1*, *dCsLOB1.2*, *dCsSWEET1.1*, and *dCsSWEET1.2*, introduced into Xcc306Δ*pthA4*, and tested for activity on citrus leaves. Xcc306Δ*pthA4* with either *dCsLOB1.1* or *dCsLOB1.2* induced *CsLOB1* expression, but did not induce *CsSWEET1*, whereas Xcc306Δ*pthA4* with *dCsSWEET1.1* or *dCsSWEET1.2* induced the expression of *CsSWEET1* but not

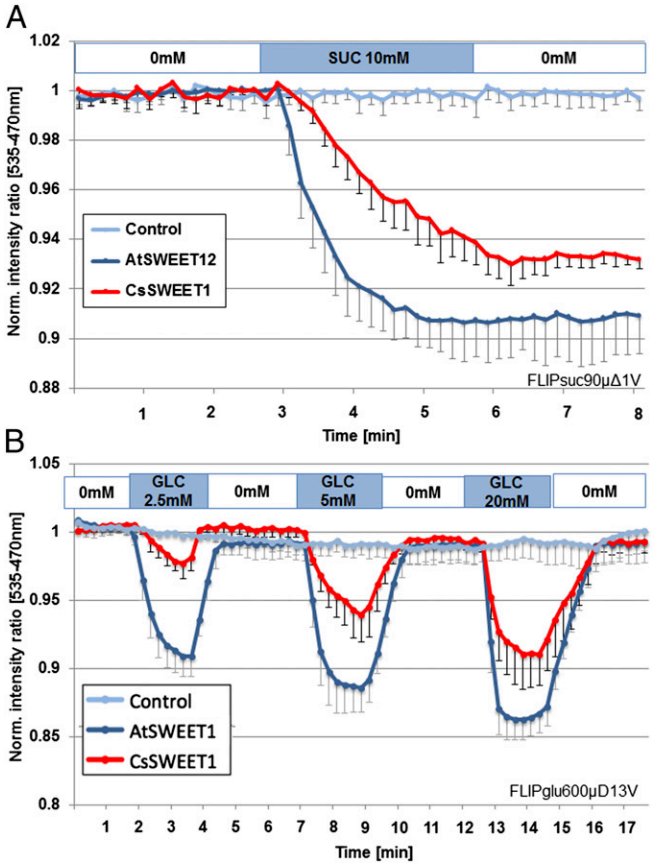

Fig. 3. Identification of CsSWEET1 substrates through HEK293T cell–FRET sensor uptake assay. Sucrose/glucose transport activity for CsSWEET1 was measured by coexpression with cytosolic FRET sucrose sensor FLIPsuc90µΔ1V (*A*) and cytosolic glucose sensor FLIPglu600µD13V (*B*) in HEK293T cells. A drop in intensity ratios reflects uptake of the indicated sugar and loss of FRET fluorescence. Individual cells were analyzed by quantitative ratio imaging of CFP and Venus emission (acquisition interval 10 s). HEK293T cells transfected with sensor only (control, light blue) or with the sensor and the *Arabidopsis* SWEET12 (suc) or SWEET1 (glc; blue) as positive controls. CsSWEET1 shows sucrose and glucose influx (red). Bars are 1 SD unit.

CsLOB1 expression (Fig. 5*B*). In parallel, the Xcc306Δ*pthA4* with the individual dTALe genes were tested for the ability to induce the promoter *uidA* reporter genes by quantitative and qualitative transient GUS assays in citrus and *N. benthamiana*. Both dTALes targeting *CsLOB1*-directed expression of the *CsLOB1* promoter, but not *CsSWEET1* promoter, and, conversely, both dTALes targeting *CsSWEET1* drove expression of the *CsSWEET1* promoter reporter genes and not the *CsLOB1* promoter fusion in citrus leaves (Fig. 5 *C* and *D*). The dTALe-complemented strains of Xcc306Δ*pthA4* were infiltrated into sweet orange and grapefruit to determine what effect the artificial effectors would have on the disease phenotype. Only inoculations of Xcc306Δ*pthA4* with either dTALe targeting *CsLOB1* resulted in pustule formation, whereas Xcc306Δ*pthA4* with *dCsSWEET1.1* or *dCsSWEET1.2* resulted in weak disease symptoms, which were similar to the response of Xcc306Δ*pthA4* alone (Fig. 6*A*). Histological analysis of tissue infected with Xcc306Δ*pthA4::dCsLOB1.1* revealed excessive cell division and proliferation (hyperplasia) similar to tissue with Xcc306Δ*pthA4::pthAw* (Fig. 6*B*) and in contrast to inoculated tissue with Xcc306Δ*pthA4*. The bacterial leaf populations were significantly higher in sweet orange leaves inoculated with Xcc306Δ*pthA4::dCsLOB1.1* compared with Xcc306Δ*pthA4* but lower than Xcc306Δ*pthA4::pthA4* (Fig. 7).

***CsLOB1* Is Target of Alternate TAL Effectors Involved in CBC.** The TAL effector genes *pthA**, *pthB*, and *pthC*, which were previously shown to be associated with pustule formation (30), were tested for the ability to induce pustule formation in Xcc306Δ*pthA4*. The complementing strains of Xcc306Δ*pthA4* with each respective gene were inoculated on sweet orange and grapefruit host to assess the ability to induce *CsLOB1* and *CsSWEET1*. The three genes, similar to *pthA4* and *pthAw*, could confer pustule formation in Xcc306Δ*pthA4* (Fig. S6*A*). PthA4, PthAw, and PthA* led to induction of both *CsSWEET1* and *CsLOB1* in both species, whereas PthB and PthC could only direct the expression of *CsLOB1*, but not *CsSWEET1*, in both species (Fig. 8).

The EBEs of all of the five TAL effectors were predicted on the basis of their contained RVDs and the DNA binding specificity (Fig. S2*A*). The predicted EBEs of both PthB and PthC were located six bases upstream of EBE_{PthA4}. The predicted EBEs of PthAw and PthA* are located at the same position as that of PthA4 (Fig. 9*A*). Xcc306Δ*pthA4::pthB* and Xcc306Δ*pthA4::pthC* strains could only direct expression of the wild-type *CsLOB1* promoter but not the truncated versions (Fig. 9*B*), which are missing three bases of the predicted EBEs for PthB and PthC. PthB and PthC also did not activate *uidA* expression with the *CsSWEET1* promoter reporter gene. Bacterial leaf populations of Xcc306Δ*pthA4::pthB* in

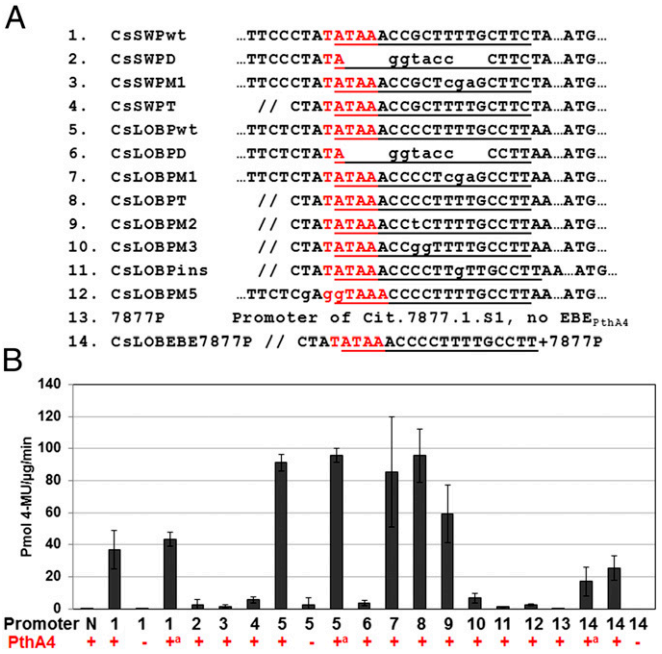

Fig. 4. PthA4 drives expression of *CsSWEET1* and *CsLOB1* promoter/*uidA* fusion genes. (*A*) Promoter constructs used in GUS transient expression assay. The predicted TAL EBEs are underlined. PD, deleted promoter; PM, mutated promoter; PT, truncated promoter; Pwt, wild-type promoter; and //, truncation. Base mutations are in lowercase letters, and red font represents putative TATAA box. Fragments including 5′ UTR and ∼100-bp coding sequences of the genes were fused to the ATG of the *uidA* coding sequence. (*B*) Transient GUS activity associated with *CsSWEET1* and *CsLOB1* promoters after inoculation with Xcc306 and derivative strains in sweet orange. *Xanthomonas* were inoculated 5 h after the inoculation with *A. tumefaciens* containing the GUS reporter constructs as indicated in *A*. N, empty vector without promoter fragment; + and –, with PthA4 and without PthA4, respectively; [a], inoculation with Xcc306Δ*pthA4::pthA4*. GUS activity was assayed 5 d after inoculation. SD values were calculated from three technical replicates of one experiment. The experiment was repeated twice with similar results.

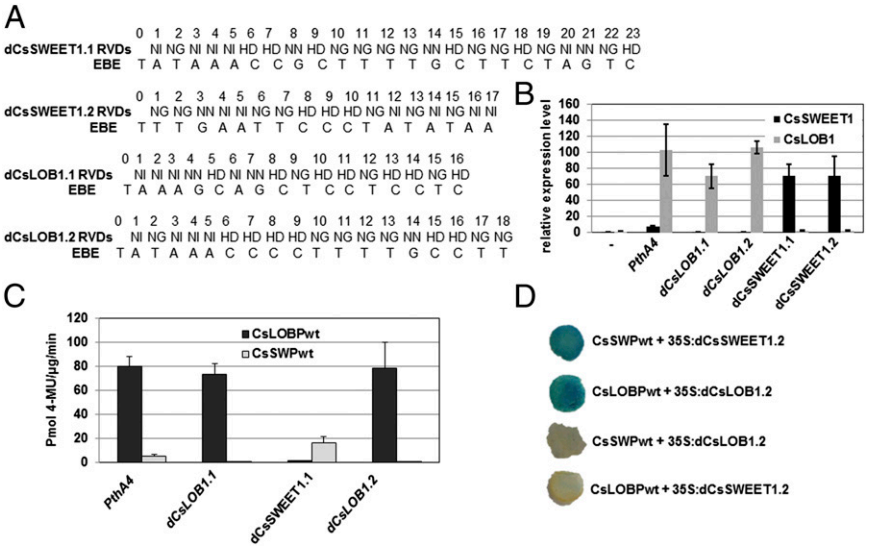

Fig. 5. dTALes-mediated induction of *CsLOB1* or *CsSWEET1*. (*A*) RVDs of dTALes and the corresponding targeted EBE sequences in the host genome. dCsSWEET1.1 targets EBE_{PthA4} in *CsSWEET1* promoter but with a 3′ extension, whereas dCsSWEET1.2 targets a sequence 13 bp upstream of the predicted EBE_{PthA4}. dCsLOB1.1 targets a sequence 33 bp downstream of EBE_{PthA4} in *CsLOB1* promoter, whereas dCsLOB1.2 is the optimized dTALe for EBE_{PthA4} in *CsLOB1* promoter (exact consensus match). (*B*) Artificial dTALes induced expression of the corresponding targeted genes. The dTALes genes were introduced into Xcc306Δ*pthA4*, and qRT-PCR analysis of host mRNA was conducted 48 h after the inoculation. Data represent the mean ± SD with three replications. (*C*) GUS activity assay using dCsSWEET1.1, dCsLOB1.1, and dCsLOB1.2 complementing Xcc306Δ*pthA4* strains. *Agrobacterium* and *Xanthomonas* were coinfiltrated into leaf tissue of sweet orange, and assays were conducted at 5 d after the infiltrations. Black columns indicate *A. tumefaciens* with CsLOBPwt::GUS constructs, gray columns indicate *A. tumefaciens* with CsSWPwt::GUS constructs. Inoculation with Xcc306Δ*pthA4*::*pthA4* was used as a positive control. (*D*) GUS staining assay in *N. benthamiana* leaves upon ectopic expression of either *dCsSWEET1.2* or *dCsLOB1.2*, respectively, using the CaMV35S promoter to drive expression. *Agrobacterium* harboring 35S:*dCsSWEET1.2* or 35S:*dCsLOB1.2* was coinfiltrated with *Agrobacterium* containing CsSWPwt or CsLOBPwt promoter/*uidA* constructs as indicated in Fig. 4*A*.

sweet orange were the same as Xcc306Δ*pthA4*::*pthA4*, and higher than the mutant Xcc306Δ*pthA4* by 9 d after infiltration (Fig. S6*B*).

In general, the induction level of *CsLOB1* in grapefruit was lower than that in sweet orange. A comparison of the promoters for *CsLOB1* and *CsSWEET1* in sweet orange and grapefruit revealed several nucleotide differences. However, the respective genes from each species have identical sequences within the predicted EBEs (Fig. S7).

***CsLOB1* Is Associated with Cell Wall-Related Gene Expression.** Based on expression analyses of inoculation with Xcc306, a high proportion of host genes are associated with cell wall metabolism (Fig. S8*A*). Six of the top 10 induced genes by PthA4 in sweet orange, for example, are predicted to be involved in cell wall metabolism (Table 1), and 12% of the genes induced greater than 16-fold after inoculation of sweet orange with Xcc306 wild type compared with the deletion mutant Xcc306Δ*pthA4* are categorized as involved in cell wall metabolism (Fig. S8*A*). However, the expression of the host genes may be due to off-target TAL effector-mediated expression. To examine the association of *CsLOB1* expression and the expression of cell wall-related genes in more detail, a select group of genes relating to expansion and wall metabolism were chosen from the most induced genes during infection by strains carrying *pthA4* and tested for induction by qRT-PCR in the presence of dCsLOB1.1. The rationale for the approach was that PthA4 and dCsLOB1.1 have different EBEs and, consequently, are unlikely to share the same set of off-target genes, and coinduced genes may be associated with *CsLOB1* expression. The approach revealed that genes for pectate lyase, extension, α-expansin, and cellulose, which were highly up-regulated by PthA4, were all found to be up-regulated with dCsLOB1.1 (Fig. 10). PthB inoculation in grapefruit was also accompanied by elevated expression of cell wall-associated genes (Fig. S8*B*). Expression of six genes was measured 36 h after inoculation with *X. citri* to determine if expression was sensitive to protein translation inhibitor cycloheximide (CHX) treatment. Transcription of TAL effector-targeted genes has been shown experimentally to be CHX-insensitive, because the transcription factor is synthesized in the bacterium and no new host translation is required (31). Addition of CHX with inoculation led to the inhibition of Cit.7877, 39387, 20509, and 2392 transcript, whereas expression of *CsLOB1* and *CsSWEET1* was expressed at high levels (Fig. 11*A*). The same four genes were also found to be elevated upon transient expression of 35S::*CsLOB1*, whereas Cs*SWEET1*, whose expression is not hypothesized to be controlled by *CsLOB1*, was not elevated (Fig. 11*B*). However, the transient overexpression of *CsLOB1* alone did not result in the formation of an observable pustule phenotype.

Discussion

Investigations into the TAL effector-mediated effects on host gene expression revealed the remarkable probing by *Xanthomonas* species for vulnerabilities in host physiology using TAL effectors. Based on the results, we propose that pustule formation involves cooption of a single host S gene *CsLOB1* in two citrus species, sweet orange and grapefruit, via any one of the PthA homologs. The results also have historical interest in that PthA of *X. citri* ssp. *citri* was one of the first T3S effectors demonstrated for being essential for virulence and the first TAL effector determined to be essential for pustule formation in CBC and with disease symptoms (20). Although PthA itself was not tested specifically in this study, the effector has the same predicted target site as PthA4 (18). Subsequently, a variety of TAL effector genes have been discovered that are required for pustule formation symptoms of CBC (30). Genes for the TAL effectors PthA4, PthAw, PthA*, PthB, and PthC from genetically diverse *Xanthomonas* strains that cause CBC restore pustule formation to the impaired strain Xcc306Δ*pthA4*. On the basis of microarray and qRT-PCR expression analyses, all PthA variants were associated with an increase in *CsLOB1* expression upon in-

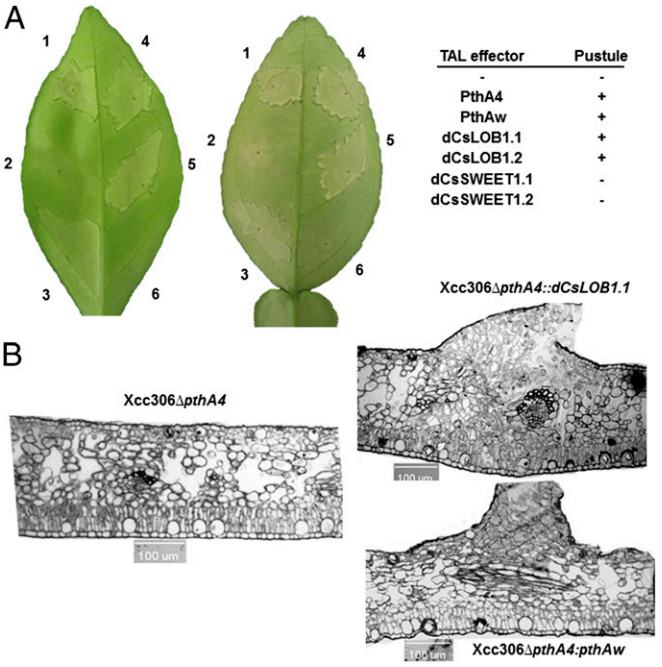

Fig. 6. dTALes targeting *CsLOB1* promoter when expressed in Xcc306Δ*pthA4* restore pustule formation in citrus. (*A*) Lesion symptoms after inoculation with strains containing natural or artificial TAL effector genes. (*Left*) Sweet orange; (*Right*) grapefruit. Leaves were inoculated with a bacterial concentration of 5×10^8 cfu/mL and photographed at 5 d after infiltration. Panels: 1, Xcc306; 2, Xcc306Δ*pthA4* (mutant); 3, Xcc306Δ*pthA4*::*dCsLOB1.1*; 4, Xcc306Δ*pthA4*::*pthA4*; 5, Xcc306Δ*pthA4*::*pthAw*; 6, Xcc306Δ*pthA4*::*dCsSWEET1.1*. The right table indicates presence or absence of the pustule symptoms with Xcc306Δ*pthA4* containing the gene for the indicated effector or Xcc306Δ*pthA4* alone. In pustule column, –, no pustule; +, pustule formation observed at 5 d. (*B*) Thin cross-section images of grapefruit leaves 5 d after inoculation with Xcc306Δ*pthA4* (*Left*), Xcc306Δ*pthA4*::*dCsLOB1.1* (*Upper Right*), and Xcc306Δ*pthA4*:*pthAw* (*Lower Right*).

fection. To further substantiate the claim and distinguish targeted from collateral and possible off-target gene inductions, dTALes were designed and targeted to unique or optimal binding sites within the *CsLOB1* promoter with the rationale that effectors targeting alternate sites are unlikely to have the same off-target sites. Only dTALes targeting *CsLOB1* restored pustule formation and enhanced bacterial growth when expressed in bacteria. The dTALes targeting another gene that was predicted to have an EBE—namely, *CsSWEET1*, did lead to *CsSWEET1* expression but did not lead to pustule formation or enhanced bacterial growth. Finally, promoter reporter assays also demonstrated that *CsLOB1* was indeed expressed in a TAL effector-dependent manner in both citrus and *N. benthamiana* expression assays, and *CsLOB1* expression was less sensitive to cycloheximide inhibition in the presence of PthA4. The predicted EBEs in *CsLOB1* promoter meet the general prediction requirements, and, for the most part, the results of experimental tests of EBE function for *CsLOB1* were consistent with predictions (32). The truncated version of the target site in *CsLOB1*, which eliminated the upstream sequences, was also functional both in citrus and *Nicotiana*. Changes in the EBE box in some instances dramatically altered expression. Noncanonical substitutions in the proximal 5′ half of the binding site had severe effects for PthA4-mediated expression compared with changes in the distal sequence of TTT, and a single base insertion, which throws the distal part out of register, also eliminated effector-mediated expression for *CsLOB1*. Changes in the respective TATAA boxes for *CsLOB1* and *CsSWEET1* eliminated expression, as might be expected for the predicted TATAA boxes for each gene. When the predicted EBE for *CsLOB1* was added to a non–EBE-containing promoter (Cit.7877.1.S1_at), the gene acquired PthA4-mediated expression ability.

The predicted EBE for PthB and PthC overlaps and starts 6 bp upstream of the EBE_{PthA4}. The arrangement is similar to the *Os11N3* promoter in rice, which contains EBE_{PthXo3} in front of the EBE_{AvrXa7} (24). The difference between PthXo3 and AvrXa7 has been postulated to result from the avoidance of triggering incompatibility in rice lines with the R gene *Xa7*. No TAL effector-dependent dominant R genes have been identified in citrus. Alternatively, PthB and PthC were isolated from *X. fuscans* ssp. *aurantifolii*, and differences may simply reflect convergence to a functional EBE. A more appropriate comparison may be to TalC, which targets an upstream site in the *Os11N3* promoter (28). *TalC* arose in strains of *X. oryzae* pv. *oryzae*, which are limited to West Africa. *TalC* may represent an independent convergence to the rice S gene *Os11N3* and not represent an adaptation to *Xa7*, which has not been deployed in West Africa.

CsLOB1 represents the third disease complex in which the natural target of a TAL effector has been identified, and, in each host species involved, a unique class of host gene was identified. With the exception of several rice S genes, the evidence linking gene induction to disease susceptibility is correlative, and, ultimately, an understanding of *CsLOB1* function in CBC, and other TAL-dependent S gene products in other disease complexes, will come from genetic and molecular/biochemical analyses of the gene and gene product. In rice, members of the SWEET gene family function as S genes for bacterial blight, and a variety of promoter sequence polymorphisms has been identified in resistant genotypes or engineered that interfere with specific TAL-effector induction of individual S genes (29, 33, 34). *CsLOB1* is a member of the plant-specific LOB family of transcription factors. A target of TAL effector AvrBs3 in pepper is *upa20*, an auxin-responsive gene for a transcription factor in the large bHLH family (22). No promoter polymorphisms have been identified in citrus or pepper cultivars, and no engineered alterations have been constructed.

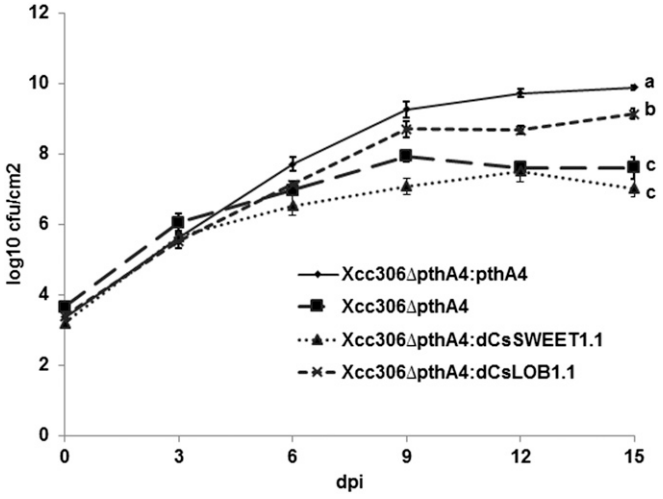

Fig. 7. dCsLOB1.1 enhances growth of Xcc306Δ*pthA4* in sweet orange. Xcc306Δ*pthA4* and Xcc306Δ*pthA4*::*dCsSWEET1.1* have reduced bacterial leaf population compared with Xcc306Δ*pthA4*::*pthA4* and Xcc306Δ*pthA4*::*dCsLOB1.1*. Leaves were inoculated at the concentration of 5×10^5 cfu /mL, and the population was measured at the time points indicated. Error bars represent 1 SD. Significance between strains was assessed at final time point at $P < 0.01$ by using Tukey–Kramer HSD test for post-ANOVA analysis. Values at 15 dpi with the same letter do not differ at the significance level of $P < 0.01$. The experiment was repeated twice with similar results.

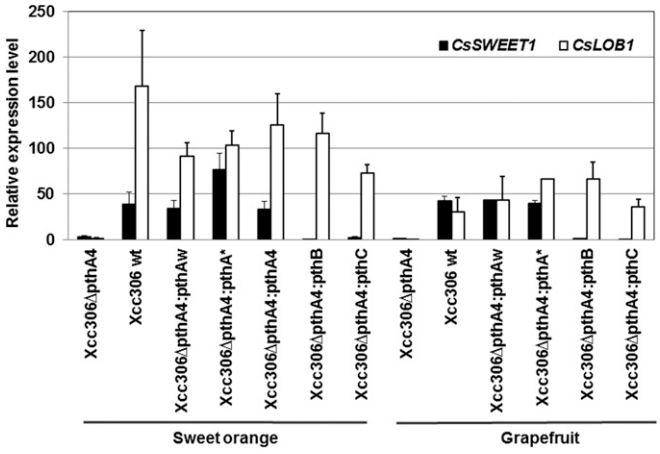

Fig. 8. Multiple TAL effectors associated with pustule formation in CBC induce *CsLOB1* and/or *CsSWEET1* in sweet orange and grapefruit. Black columns represent the expression values of *CsSWEET1*, and white columns indicate expression values of *CsLOB1*. RNA was prepared 48 h after inoculation. Strains with genes for PthB and PthC did not induce *CsSWEET1* in either species. Data represent the mean ± SD of three replications.

Further insight of *CsLOB1* involvement will come from characterization of the normal function of the gene. The plant-specific LOB domain family is composed of a conserved DNA-binding Cys repeat motif ($CX_2CX_6CX_3C$), an invariant glycine residue, and a coiled-coil Leu zipper-like motif ($LX_6LX_3LX_6L$), the latter of which often functions in protein–protein interactions (35). Although the specific functions of CsLOB1 are unknown, previous studies have revealed that LOB domain proteins are involved in the regulation of lateral organ development, anthocyanin and nitrogen metabolism, and are responsive to phytohormones and environmental stimuli such as auxin, cytokinin, gibberellin, brassinosteroid, and salinity or glucose (36, 37). One member of the LOB domain family, AtLBD18, was reported to bind with the promoter of *EXPANSIN14*, a gene involved in cell wall loosening (38). Recently, the *Arabidopsis* LOB family protein LBD20 was proposed as a host S gene for the fungal pathogen *Fusarium oxysporum*, functioning in the jasmonate signaling pathway (39). *AtLBD20* was induced by *F. oxysporum*, and the overexpression of *LBD20* was correlated with increased susceptibility to infection and reduced the expression of JA-regulated genes *VEGETATIVE STORAGE PROTEIN2* (*VSP2*) and *THIONIN2.1* (*Thi2.1*). Other LOB domain family genes were also detected to be responsive to fungal and root pathogens from public *Arabidopsis* array data (40). Here, we showed that *CsLOB1* expression is associated with expression of numerous cell wall-related enzymes, indicating a possible function in cell wall biochemistry. Expression of four of the genes was shown to be sensitive to cycloheximide inhibition, whereas expression of the TAL-dependent genes *CsLOB1* and *CsSWEET1* were not sensitive. Furthermore, transient expression of *CsLOB1* led to elevated levels of the four genes, whereas *CsSWEET1* remained below detection; however, transient expression of *CsLOB1* did not result in observable pustule formation, possibly as a result of the low percentage of *Agrobacterium*-transfected cells. Further functional analyses of *CsLOB1* and associated genes will be required to establish a direct causal relationship to the virulence of Xcc and expression of host genes other than *CsLOB1*. Pustule formation in CBC involves both hyperplasia and hypertrophy of cells (41, 42). It is interesting in this regard that an interaction between an LOB and bHLH transcription factor was reported for *Arabidopsis* (43). Although correlative, transient expression of *upa20*, a member of the bHLH family, has been reported to induce cell hypertrophy, one of the phenotypes of pepper infection by *Xanthomonas axonopodis* pv. *vesicatoria* containing *avrBs3* (22). Future insights into CsLOB1 and UPA20 may reveal targeting a common pathway at different control points for diseases involving *X. axonopodis* pv. *vesicatoria*, *X. citri* ssp. *citri*, and *X. fuscans* ssp. *aurantifolii*.

The results for the candidate EBEs in *CsSWEET1* were more complex. Only the longer promoter construct supported TAL effector-mediated induction. Truncation of the *CsSWEET1* promoter to include only the TATAA box region could not support expression either in citrus or *N. benthamiana*. At the same time, a change similar to the one conducted for *CsLOB1* in the distal TTT sequence of EBE site A also resulted in loss of expression in transient assays, and both naturally occurring effectors PthB and PthC directed *CsLOB1* but not *CsSWEET1* expression. Binding to the *CsSWEET1* promoter may, therefore, be weak, and expression may be due to multiple binding sites, including ones upstream or more complex interactions. No evidence was found supporting a major function for the SWEET gene *CsSWEET1* in CBC, although a function in CBC could not be ruled out with certainty. The gene is a member of another transporter clade from which no S gene in rice has been identified. Rice-susceptible SWEET genes *OsSWEET11*and *OsSWEET14*, which are in clade III, preferentially mediated efflux of sucrose over glucose, whereas *CsSWEET1* is in clade I with *AtSWEET1* that has been shown to predominantly transport several hexoses (44). All of the clade III OsSWEETs but not the other SWEET paralogs in rice can, potentially, condition host susceptibility and *X. oryzae* pv. *oryzae* virulence (45). Why, in rice, the type of transporter is important for susceptibility is unknown. However, *CsSWEET1* shows TAL effector-dependent expression for PthA4, PthAw, and PthA*, and full complementation of bacterial growth in citrus leaves was not attained with the *dCsLOB1.1* despite apparent robust expression of *CsLOB1*. The question remains as to whether expression of

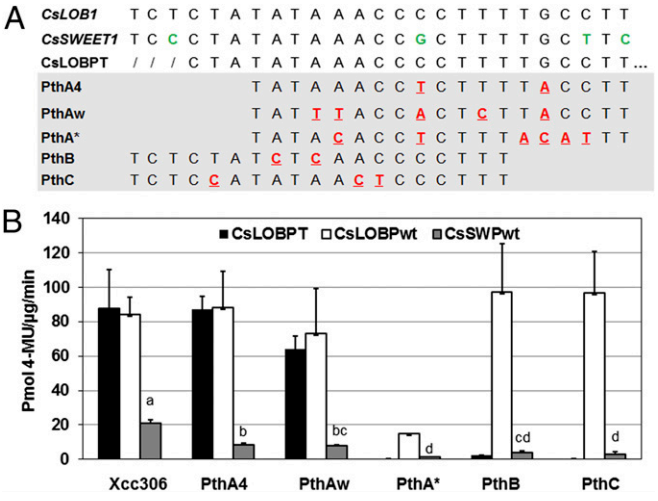

Fig. 9. PthB and PthC drive *CsLOB1* promoter, but not *CsSWEET1* promoter, expression. (*A*) Consensus EBEs of PthA4, PthAw, PthA*, PthB, and PthC (in gray) and the corresponding nucleotide sequences are depicted in the *CsLOB1* and *CsSWEET1* promoters from sweet orange. Mismatches between predicted EBE and *CsLOB1* promoter are indicated in bold red font and underlined; different bases in *CsSWEET1* promoter compared with that of *CsLOB1* are in green font. (*B*) GUS transient assays in sweet orange with the coinoculation of Xcc306 or derivative strains and *A. tumefaciens* harboring promoter/*uidA* fusion genes listed in Fig. 4*A*. Each set of columns is labeled with the specific TAL effector produced by the corresponding gene in strain Xcc306Δ*pthA4*. Data bars represent the mean ± SD with three technical replicates of one experiment. The experiment was repeated twice with similar results. Columns for CsSWPwt with the same lowercase letters do not differ from each other at the significance level of $P < 0.05$ using the Tukey test.

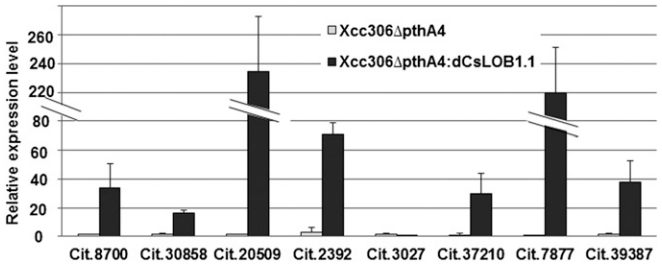

Fig. 10. Cell wall-related genes are coinduced by synthetic TAL effectors that target *CsLOB1*. Representative cell expansion or wall-related metabolism genes in sweet orange were activated by Xcc306Δ*pthA4::dCsLOB1.1* in comparison with Xcc306Δ*pthA4*. Quantitative RT-PCR was conducted on host mRNA using gene-specific primers at 48 h after the infiltration. Expression values were normalized to housekeeping gene *EF1α*. The probe sets are labeled and annotated as follows: Cit.8700, Cit.8700.1.S1_at, extension; Cit.30858, Cit.30858.1.S1_at, expansin; Cit. 20509, Cit.20509.1.S1_at, pectate lyase; Cit. 2392, Cit.2392.1.S1_at, acidic cellulose; Cit. 3027, Cit.3027.1.S1_s_at, *CsSWEET1*; Cit. 37210, Cit.37210.1.S1_at, *CsLOB1*; Cit. 7877, Cit.7877.1.S1_at, expansin; Cit. 39387, Cit.39387.1.S1_at, pectate lyase.

CsSWEET1 or other host genes represents more complex virulence adaptations on the part of the bacteria and TAL effector-mediated expression.

The EBEs of TAL effector have been proposed as effective tools to control the disease. By combining the natural EBEs of multiple TAL effectors from three distinct R genes or adding artificial EBEs of corresponding TAL effectors into one complex R gene promoter, the engineered R gene was induced by these effectors and conferred broader spectrum disease resistance (46, 47). Although no major R genes have yet been described in citrus, the well-characterized *avr* gene *AvrGf1* may reflect the presence of a potential R gene in grapefruit and sweet orange (3). Alternatively, we may engineer the EBEs identified in *CsLOB1* to drive the expression of *AvrGf1* and transform into grapefruit or sweet orange; the *AvrGf1* will be ectopically activated in plant when it encounters most of the canker-causing xanthomonads; and the encoded AvrGf1 can be recognized by the potential R protein and trigger a hypersensitive response (48). Another compelling approach using TAL effector-targeted S gene to control disease is reported by Li et al. (34), who mutated the EBEs of *Os11N3* in rice by transcription activator-like effector nuclease-based cleavage and gained transgenic rice lines conferring resistance to *X. oryzae* pv. *oryzae* that contained TAL effectors AvrXa7 and PthXo3; *CsLOB1* is a good candidate for this approach in that it is targeted by several TAL effectors and only one single mutation in EBEs region is required to obtain broad spectrum plant resistance to most kinds of citrus canker.

Materials and Methods

Plant Material, Bacterial Strains, and Plasmids. Growth conditions of plants and bacteria are described in *SI Materials and Methods*. The plasmids and bacterial strains used in this study are list in Table S1.

Mutagenesis of *pthAs* in Xcc306. The site-directed gene deletion process was described in *SI Materials and Methods*.

Bacterial Growth *in Planta*. For the population of bacteria strains in citrus plants, one leaf disk with 1 cm^2 of the inoculated area was taken and macerated in sterile tap water; after serial dilutions, 50 μL were plated on nutrient agar medium and incubated at 28 °C for 3 d. The colony counts were calculated to determine the internal populations. Each experiment was repeated three times.

Microarray Analyses and TAL Effectors Target Search. The microarray was conducted and analyzed as described in *SI Materials and Methods*. Genes with a $P \leq 0.01$ were considered as differentially expressed genes at a statistically significant level. The 1,000-bp upstream sequences of selected genes were obtained from Phytozome (www.phytozome.org/citrus.php), and the regions were scanned by Target Finder using RVD sequences of PthA4 and PthAw (49).

Designer TALe Construction. Four types of repeats encoding the RVDs NI, NN, NG, and HD that correspond to the respective nucleotide A, G, T, and C were used to assemble the repeat domains of the artificial dTALes. The description of library repeats and protocols involving Golden Gate cloning strategy were as described previously (50).

FRET Analysis in HEK293T Cells. HEK293T cells were cotransfected with the sensors FLIPsuc90μΔ1V plus AtSWEET12 (as positive control for sucrose uptake) and FLIPglu600μD13V plus AtSWEET1 (as positive control for glucose uptake) or CsSWEET1 in six-well plates, and perfusion experiments were performed as described previously (51). HEK293T/FLIPsuc90mΔ1V cells were perfused with medium, followed by a pulse of 10 mM sucrose, whereas HEK293T/FLIPglu600μD13V cells were perfused with medium, followed by a pulse of 2.5–5–20 mM glucose.

Quantitative, Semiquantitative RT-PCR Analyses and GUS Assays. Citrus leaves were syringe-infiltrated with bacterial suspensions at 5×10^8 cfu/mL. For cycloheximide treatment, the Xcc306 bacterial suspensions containing 100 μM cycloheximide were used, and the leaf tissues were harvested 36 h after

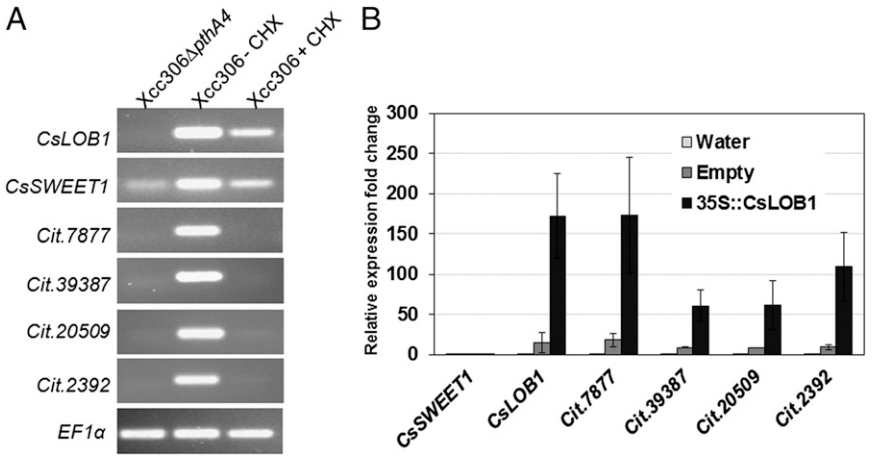

Fig. 11. Cell wall-related gene expression is sensitive to cycloheximide (CHX) and associated with transient *CsLOB1* expression. (*A*) Semiquantitative RT-PCR at 36 h after the infiltration of mutant Xcc306Δ*pthA4* and wild-type Xcc306 in the presence (+) or absence (–) of CHX. (*B*) Quantitative RT-PCR assays were conducted 6 d after infiltration of *Agrobacterium* with 35S::*CsLOB1* or empty vector. Expression values were calculated in relation to water infiltration. The representative cell wall-related genes were a subset of genes used in Fig. 10. Error bars represent 1 SD. Values between treatments were normalized to the housekeeping gene *EF1α*.

inoculation. Total RNA was extracted by using TRIzol Reagent (Ambion) following the manufacturer's instruction. The RNA was subjected to DNase I treatment and first-strand cDNA synthesis by using the ProtoScript AMV First Strand cDNA Synthesis Kit (NEB); two-step real-time PCR was performed using Real Master Mix SYBR Rox (5 PRIME). The gene-specific primer sequences are listed in Table S2. The elongation factor gene *EF1α* was used as endogenous control. The $2^{-\Delta\Delta Ct}$ method was used for relative quantification. The quantitative and qualitative GUS assays were described in *SI Materials and Methods*.

ACKNOWLEDGMENTS. We thank Ms. Haiyan Huang [Kansas State University (KSU)] for technical assistance; Dr. David Moore, Prem Singh Thapa Chetri, and Joseph Heppert of the University of Kansas Imaging Facility; the advice of Drs. Brian J. Staskawicz and Becky Bart (University of California, Berkeley) on Southern hybridization; Drs. Alina Akhunova, Hanquan Liang, and Yanni Lun of the KSU Integrated Genomics Facility; and Dr. Dean Gabriel (University of Florida) for providing several TAL effector clones. This project was supported by the Kansas Agriculture Experiment Station, National Research Initiative Competitive Grants Program Grant 2012-67013-19383 from the US Department of Agriculture (USDA) National Institute of Food and Agriculture (to F.F.W., J.B.J., N.W., and W.B.F.), Grants DBI-0820831 and IOS-1238189 from the Plant Genome Research Program of the National Science Foundation (to F.F.W. and B.Y.), and USDA Cooperative State Research, Education, and Extension Service Special Citrus Canker Grant Project 2011-73402 (to N.W. and J.B.J.).

1. Verniere C, et al. (1998) Characterization of phenotypically distinct strains of *Xanthomonas axonopodis* pv. *citri* from Southwest Asia. *Eur J Plant Pathol* 104(5): 477–487.
2. Sun X, et al. (2004) Detection and characterization of a new strain of citrus canker bacteria from key Mexican lime and Alemow in South Florida. *Plant Dis* 88(11): 1179–1188.
3. Rybak M, Minsavage GV, Stall RE, Jones JB (2009) Identification of *Xanthomonas citri* ssp. *citri* host specificity genes in a heterologous expression host. *Mol Plant Pathol* 10(2):249–262.
4. Gottwald TR, Graham JH (2005) Citrus canker. *The Plant Health Instructor*, 10.1094/PHI-I-2000-1002-01.
5. Ollitrault P, et al. (2012) A reference genetic map of *C. clementina* hort. ex Tan.; citrus evolution inferences from comparative mapping. *BMC Genomics* 13:593.
6. Xu Q, et al. (2013) The draft genome of sweet orange (*Citrus sinensis*). *Nat Genet* 45(1):59–66.
7. Cernadas RA, Camillo LR, Benedetti CE (2008) Transcriptional analysis of the sweet orange interaction with the citrus canker pathogens *Xanthomonas axonopodis* pv. *citri* and *Xanthomonas axonopodis* pv. *aurantifolii*. *Mol Plant Pathol* 9(5):609–631.
8. Fu XZ, Gong XQ, Zhang YX, Wang Y, Liu JH (2012) Different transcriptional response to *Xanthomonas citri* subsp. *citri* between kumquat and sweet orange with contrasting canker tolerance. *PLoS ONE* 7(7):e41790.
9. da Silva AC, et al. (2002) Comparison of the genomes of two *Xanthomonas* pathogens with differing host specificities. *Nature* 417(6887):459–463.
10. Moreira LM, et al. (2010) Novel insights into the genomic basis of citrus canker based on the genome sequences of two strains of *Xanthomonas fuscans* subsp. *aurantifolii*. *BMC Genomics* 11:238.
11. Jalan N, et al. (2013) Complete genome sequence of *Xanthomonas citri* subsp. *citri* strain A^{w}12879, a restricted host-range citrus canker causing bacterium. *Genome Announc* 1(3):e000235-13.
12. Yan Q, Wang N (2012) High-throughput screening and analysis of genes of *Xanthomonas citri* subsp. *citri* involved in citrus canker symptom development. *Mol Plant Microbe Interact* 25(1):69–84.
13. Figueiredo J, Minsavage G, Graham J, White F, Jones J (2011) Mutational analysis of type III effector genes from *Xanthomonas citri* subsp. *citri*. *Eur J Plant Pathol* 130(3): 339–347.
14. Laia ML, et al. (2009) New genes of *Xanthomonas citri* subsp. *citri* involved in pathogenesis and adaptation revealed by a transposon-based mutant library. *BMC Microbiol* 9:12.
15. Brunings AM, Gabriel DW (2003) *Xanthomonas citri*: Breaking the surface. *Mol Plant Pathol* 4(3):141–157.
16. Bogdanove AJ, Schornack S, Lahaye T (2010) TAL effectors: Finding plant genes for disease and defense. *Curr Opin Plant Biol* 13(4):394–401.
17. Hann DR, Gimenez-Ibanez S, Rathjen JP (2010) Bacterial virulence effectors and their activities. *Curr Opin Plant Biol* 13(4):388–393.
18. Boch J, et al. (2009) Breaking the code of DNA binding specificity of TAL-type III effectors. *Science* 326(5959):1509–1512.
19. Moscou MJ, Bogdanove AJ (2009) A simple cipher governs DNA recognition by TAL effectors. *Science* 326(5959):1501.
20. Swarup S, Yang Y, Kingsley MT, Gabriel DW (1992) An *Xanthomonas citri* pathogenicity gene, pthA, pleiotropically encodes gratuitous avirulence on nonhosts. *Mol Plant Microbe Interact* 5(3):204–213.
21. Duan Y, Castaneda A, Zhao G, Erdos G, Gabriel D (1999) Expression of a single, host-specific, bacterial pathogenicity gene in plant cells elicits division, enlargement, and cell death. *Mol Plant Microbe Interact* 12(6):556–560.
22. Kay S, Hahn S, Marois E, Hause G, Bonas U (2007) A bacterial effector acts as a plant transcription factor and induces a cell size regulator. *Science* 318(5850):648–651.
23. Yang B, Sugio A, White FF (2006) *Os8N3* is a host disease-susceptibility gene for bacterial blight of rice. *Proc Natl Acad Sci USA* 103(27):10503–10508.
24. Antony G, et al. (2010) Rice *xa13* recessive resistance to bacterial blight is defeated by induction of the disease susceptibility gene *Os-11N3*. *Plant Cell* 22(11):3864–3876.
25. Chen LQ, et al. (2010) Sugar transporters for intercellular exchange and nutrition of pathogens. *Nature* 468(7323):527–532.
26. Römer P, et al. (2007) Plant pathogen recognition mediated by promoter activation of the pepper *Bs3* resistance gene. *Science* 318(5850):645–648.
27. Schornack S, Minsavage GV, Stall RE, Jones JB, Lahaye T (2008) Characterization of AvrHah1, a novel AvrBs3-like effector from *Xanthomonas gardneri* with virulence and avirulence activity. *New Phytol* 179(2):546–556.
28. Yu Y, et al. (2011) Colonization of rice leaf blades by an African strain of *Xanthomonas oryzae* pv. *oryzae* depends on a new TAL effector that induces the rice nodulin-3 *Os11N3* gene. *Mol Plant Microbe Interact* 24(9):1102–1113.
29. Sugio A, Yang B, Zhu T, White FF (2007) Two type III effector genes of *Xanthomonas oryzae* pv. *oryzae* control the induction of the host genes *OsTFIIAgamma1* and *OsTFX1* during bacterial blight of rice. *Proc Natl Acad Sci USA* 104(25):10720–10725.
30. Al-Saadi A, et al. (2007) All five host-range variants of *Xanthomonas citri* carry one *pthA* homolog with 17.5 repeats that determines pathogenicity on citrus, but none determine host-range variation. *Mol Plant Microbe Interact* 20(8):934–943.
31. Strauss T, et al. (2012) RNA-seq pinpoints a *Xanthomonas* TAL-effector activated resistance gene in a large-crop genome. *Proc Natl Acad Sci USA* 109(47):19480–19485.
32. Grau J, et al. (2013) Computational predictions provide insights into the biology of TAL effector target sites. *PLOS Comput Biol* 9(3):e1002962.
33. Chu Z, et al. (2006) Promoter mutations of an essential gene for pollen development result in disease resistance in rice. *Genes Dev* 20(10):1250–1255.
34. Li T, Liu B, Spalding MH, Weeks DP, Yang B (2012) High-efficiency TALEN-based gene editing produces disease-resistant rice. *Nat Biotechnol* 30(5):390–392.
35. Shuai B, Reynaga-Peña CG, Springer PS (2002) The lateral organ boundaries gene defines a novel, plant-specific gene family. *Plant Physiol* 129(2):747–761.
36. Majer C, Hochholdinger F (2011) Defining the boundaries: Structure and function of LOB domain proteins. *Trends Plant Sci* 16(1):47–52.
37. Gendron JM, et al. (2012) Brassinosteroids regulate organ boundary formation in the shoot apical meristem of *Arabidopsis*. *Proc Natl Acad Sci USA* 109(51):21152–21157.
38. Kim J, Lee HW (2013) Direct activation of EXPANSIN14 by LBD18 in the gene regulatory network of lateral root formation in *Arabidopsis*. *Plant Signal Behav* 8(2): e22979.
39. Thatcher LF, Powell JJ, Aitken EA, Kazan K, Manners JM (2012) The lateral organ boundaries domain transcription factor LBD20 functions in Fusarium wilt susceptibility and jasmonate signaling in *Arabidopsis*. *Plant Physiol* 160(1):407–418.
40. Thatcher LF, Kazan K, Manners JM (2012) Lateral organ boundaries domain transcription factors: New roles in plant defense. *Plant Signal Behav* 7(12):1702–1704.
41. Lawson R, Dienelt M, Civerolo E (1989) Histopathology of *Xanthomonas campestris* pv *citri* from Florida and Mexico in wound-inoculated detached leaves of *Citrus* aurantifolia: Light and scanning electron microscopy. *Phytopathology* 79(3):329–335.
42. Swarup S, Defeyter R, Brlansky R, Gabriel D (1991) A pathogenicity locus from *Xanthomonas citri* enables strains from several pathovars of *Xanthomonas campestris* to elicit cankerlike lesions on citrus. *Phytopathology* 81(7):802–809.
43. Husbands A, Bell EM, Shuai B, Smith HM, Springer PS (2007) LATERAL ORGAN BOUNDARIES defines a new family of DNA-binding transcription factors and can interact with specific bHLH proteins. *Nucleic Acids Res* 35(19):6663–6671.
44. Chen LQ, et al. (2012) Sucrose efflux mediated by SWEET proteins as a key step for phloem transport. *Science* 335(6065):207–211.
45. Streubel J, et al. (2013) Five phylogenetically close rice SWEET genes confer TAL effector-mediated susceptibility to *Xanthomonas oryzae* pv. *oryzae*. *New Phytol* 200(3): 808–819.
46. Römer P, Recht S, Lahaye T (2009) A single plant resistance gene promoter engineered to recognize multiple TAL effectors from disparate pathogens. *Proc Natl Acad Sci USA* 106(48):20526–20531.
47. Hummel AW, Doyle EL, Bogdanove AJ (2012) Addition of transcription activator-like effector binding sites to a pathogen strain-specific rice bacterial blight resistance gene makes it effective against additional strains and against bacterial leaf streak. *New Phytol* 195(4):883–893.
48. Shantharaj D, et al. (2013) Deciphering specificities of TAL effectors in *Xanthomonas citri* and prospects in citrus. *Phytopathology* 103(Suppl 2):S2.131.
49. Doyle EL, et al. (2012) TAL effector-nucleotide targeter (TALE-NT) 2.0: Tools for TAL effector design and target prediction. *Nucleic Acids Res* 40(Web server issue):W117–W122.
50. Li T, Yang B (2013) TAL effector nuclease (TALEN) engineering in enzyme engineering. *Methods Mol Biol* 978:63–72.
51. Hou BH, et al. (2011) Optical sensors for monitoring dynamic changes of intracellular metabolite levels in mammalian cells. *Nat Protoc* 6(11):1818–1833.

Supporting Information

Hu et al. 10.1073/pnas.1313271111

SI Materials and Methods

Plants and Bacteria Growth Conditions. The citrus plants grapefruit (*Citrus paradisi*), cultivar (cv.) Duncan, and sweet orange (*Citrus sinensis*), cv. Valencia, were kept in a glasshouse at the Florida Department of Agriculture and Consumer Services, Division Plant Industry, Gainesville, FL, or in a quarantine greenhouse facility at the Citrus Research and Education Center, Lake Alfred, FL. The temperature ranged between 25 and 30 °C with a 12/12-h photoperiod. Plants were pruned routinely to stimulate new leaf growth. Leaves chosen for infiltration were 14–21 d old and fully expanded. Plants were kept in the growth room at 28 ± 2 °C with 16 h light and 40–60% humidity after the inoculation. Strains of *Xanthomonas* were grown at 28 °C on nutrient agar (NA), *Agrobacterium tumefaciens* was cultivated at 28 °C on yeast extract peptone plates, *Escherichia coli* was grown at 37 °C in LB. Antibiotics were used at the following concentrations: ampicillin, 100 μg/mL; kanamycin, 50 μg/mL; rifamycin SV, 100 μg/mL; spectinomycin, 100 μg/mL; tetracycline, 12.5 μg/mL; gentamicin, 10 μg/mL; and chloramphenicol, 30 μg/mL.

Deletion of *pth Genes* in Xcc306. To delete *pthA* genes from the genome DNA of Xcc306, each *pthA* gene, including the flanking sequences, was amplified; the central regions of them were deleted by BamHI and self-ligated. The deleted *pthA* gene fragments were excised with ApaI and SpeI from pGEMT clone for ligation into suicide vector pOK1. Restriction enzymes, T4 DNA ligase, and Taq DNA polymerase (Promega) were used according to the manufacturer recommendations. Through triparental (donor, recipient, and helper) conjugation, the *pthA* knocked-out strains were produced as described by Huguet et al. (1). For the double, triple, and quadruple mutants, single, double, and triple mutants were used as recipients, respectively. The mutants were confirmed by PCR with single *pthA*-specific primer pairs and Southern hybridization analyses with *pthA* fragment.

Microarray Analyses. Xcc strains Xcc306 (wild-type) and Xcc306Δ*pthA4* (mutant) were used to inoculate sweet orange (*Citrus sinensis*) at the concentration of 5×10^8 cfu/mL. The leaves were harvested 6, 48, and 120 h after inoculation for RNA isolation. Three biological replicates were conducted for each strain per time point. RNA extraction was performed by using RNeasy Plant Mini Kit (Qiagen), and the quantity and quality of RNA were determined on a ND-8000 NanoDrop spectrophotometer (NanoDrop Technologies). Microarray was conducted using Affymetrix array containing 33,000 citrus-related species genes and is commercially available. Labeling, hybridization, washing, scanning, and data analysis were performed at the Interdisciplinary Center for Biotechnology Research facility at the University of Florida in Gainesville or the Integrated Genomics Facility at Kansas State University. Statistical tests were performed using BioConductor statistical software, open source software based on the R programming language (www.bioconductor.org/). Robust multichip analysis was used for normalizing the raw data. Differential expression analysis was carried out using a linear modeling approach and the empirical Bayes statistics as implemented in the Limma package.

GUS Reporter and Ectopic Expression Gene Construction. Sequences 600 bp upstream of *CsSWEET1* and *CsLOB1* coding sequences were amplified from sweet orange or grapefruit genome DNA using primers derived from expression sequence tags and genomic sequences retrieved from the Phytozome Web site (www.phytozome.net). Promoter derivatives were constructed by amplification with appropriate primers (listed in Table S2). The promoter fragments were digested with BamHI and HindIII and fused with *uidA* gene in pBI101. The constructs were transformed into *Agrobacterium* strain EHA101. To express *pthA4* and *pthAw* ectopically, the amplified genes were inserted after 35S CaMV promoter and before the NOS terminator in vector pUC118/35S polylinker at the ApaI and XhoI sites. The constructs were then digested with HindIII and XbaI and ligated into pCAMBIA2200 and introduced into *Agrobacterium* strain LBA4404.

β-Glucuronidase Assays. For transient β-glucuronidase (GUS) expression in citrus leaves, *Agrobacterium* was suspended in solution containing 10 mM MgCl2, 10 mM Mes (pH 5.6), and 100 μM acetosyringone with concentration OD_{600} = 0.8 and infiltrated into sweet orange. Five hours after inoculation with *Agrobacterium*, *Xanthomonas* at an OD_{600} of 0.3 was infiltrated at the same area. Five days after inoculation with *Xanthomonas*, the GUS activities were measured (2). For the transient expression in *Nicotiana benthamiana*, two *Agrobacterium* suspensions were mixed at ratio of 1:1, and the GUS assay was performed 3 d after infiltration. For quantitative GUS assay, one leaf disk (1 cm diameter) was grounded with 400 μL GUS extraction buffer [50 mM $NaPO_4$ (pH 7.0), 1 mM Na_2EDTA, 0.1% SDS, 0.1% Triton X-100, 10 mM DTT]. The ground material was centrifuged at 4 °C for 15 min at top speed in a tabletop centrifuge. Twenty-five microliters of the supernatant was mixed with 225 μL GUS assay buffer (GUS extraction buffer supplied with 0.44 mg/mL 4-methyl umbelliferyl β-D-glucuronide) and kept at 37 °C for 1 h. The reaction was stopped with 0.2 M Na_2CO_3. Product formation was measured spectrophotometrically using a plate reader (CytoFluor II) at 360 nm (excitation) and 460 nm (emission) with 4-methyl-umbelliferon dilutions as standard. Protein quantification was performed by Bradford assay (Bio-Rad). For qualitative GUS assay, one fresh leaf disk was put into GUS staining buffer [50 mM $NaPO_4$ (pH 7.0), 0.1% Triton X-100, 10 mM EDTA, 1 mM $K_3Fe(CN)_6$, 1 mM $K_4Fe(CN)_6$, 0.5 mg/mL X-gluc] and incubated at 37 °C overnight. The discs were then destained in ethanol.

Phylogenic Analyses. The phylogenic relationship was inferred using the neighbor-joining method (3). The optimal tree with the sum of branch length = 5.24593591 is shown. The tree is drawn to scale, with branch lengths in the same units as those of the evolutionary distances used to infer the phylogenetic tree. The evolutionary distances were computed using the Poisson correction method (4) and are in the units of the number of amino acid substitutions per site. The analysis involved 18 amino acid sequences. All positions containing gaps and missing data were eliminated. A total of 204 positions were included in the final dataset. Evolutionary analyses were conducted with MEGA5 software package (5).

1. Huguet E, Hahn K, Wengelnik K, Bonas U (1998) hpaA mutants of *Xanthomonas campestris* pv. *vesicatoria* are affected in pathogenicity but retain the ability to induce host-specific hypersensitive reaction. *Mol Microbiol* 29(6):1379–1390.

2. Figueiredo JF, et al. (2011) *Agrobacterium*-mediated transient expression in citrus leaves: A rapid tool for gene expression and functional gene assay. *Plant Cell Rep* 30(7): 1339–1345.

3. Saitou N, Nei M (1987) The neighbor-joining method: A new method for reconstructing phylogenetic trees. *Mol Biol Evol* 4(4):406–425.
4. Zuckerkandl E, Pauling L; Bryson V, Vogel HJ (1965) Evolutionary divergence and convergence in proteins. *Evolving Genes and Proteins* (Academic, New York), pp 97–166.
5. Tamura K, et al. (2011) MEGA5: Molecular evolutionary genetics analysis using maximum likelihood, evolutionary distance, and maximum parsimony methods. *Mol Biol Evol* 28(10):2731–2739.

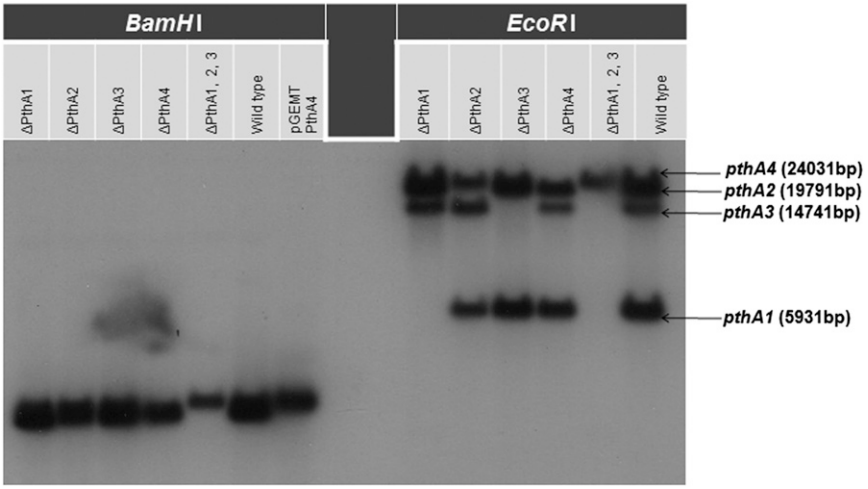

Fig. S1. Southern blot analysis of Xcc306 transcription activator-like (TAL) effector genes in deletion mutants. The genome DNA was digested with BamHI and EcoRI. The filter was photographed after 120 min of exposure. The induction of *CsSWEET1* and *CsLOB1* in grapefruit was eliminated following challenge with strain Xcc306Δ*pthA4* (*Left*, black columns) in comparison with infiltration with complemented strain Xcc306Δ*pthA4::pthAw* (gray columns). Quantitative RT-PCR was performed at 120 h after the inoculation. Data represent the mean ± SD.

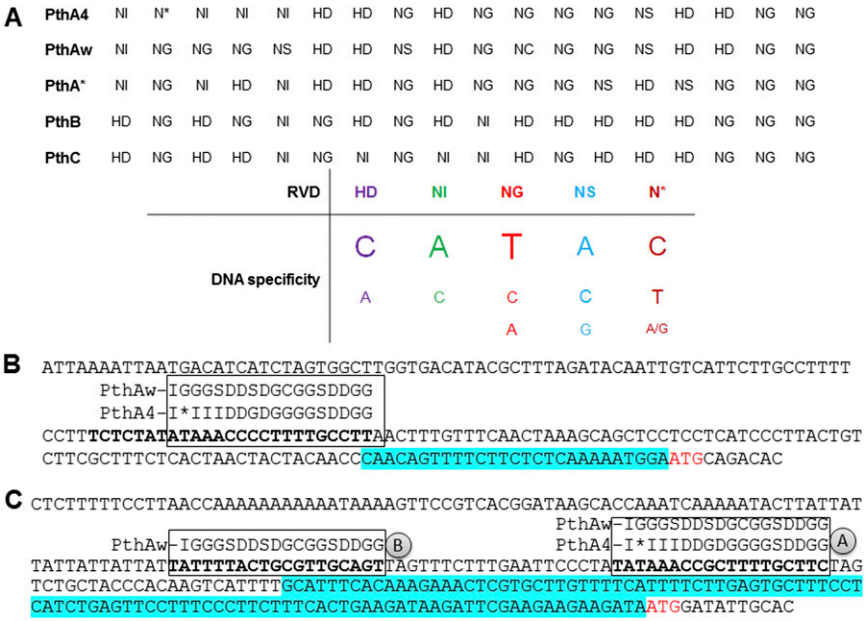

Fig. S2. The repeat variable diresidues (RVDs) of five major TAL effectors that determine pustule formation in citrus bacterial canker and corresponding candidate EBEs in the promoters of *CsLOB1* and *CsSWEET1*. (*A*) Each of the TAL effector contains 18 RVDs (12th and 13th repeat-variable diresidue). An asterisk indicates the missing 13th amino acid. The TAL code is on the basis of Grau et al. (1). Briefly, each RVD preferentially associates with one or more of the four nucleotides; the bigger font of the nucleotide, the greater the association with the particular nucleotide. The code frequency of association is then used to predict potential TAL effector binding sites within a given sequence. (*B*) Promoter of *CsLOB1*. (*C*) Promoter of *CsSWEET1*. RVDs of the TAL effector and the predicted targets are in the same box. RVD abbreviations in *B*: I, NI; G, NG; S, NS; D, HD; *, N*. The predicted EBE of each TAL effector is in bold font; 5′ UTRs are highlighted, and the coding start site (ATG) is in red.

1. Grau J, et al. (2013) Computational predictions provide insights into the biology of TAL effector target sites. *PLOS Comput Biol* 9(3):e1002962.

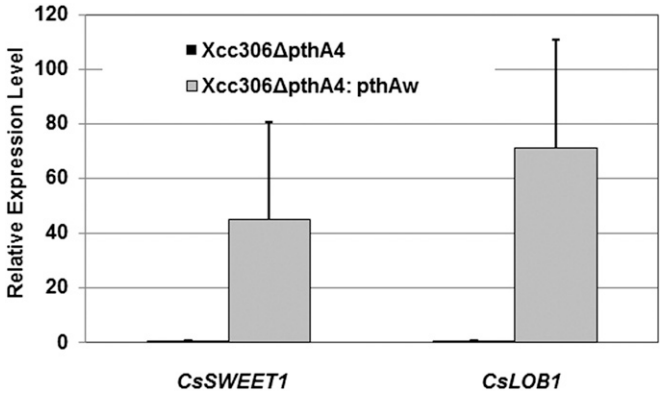

Fig. S3. *CsSWEET1* and *CsLOB1* are induced by PthAw in grapefruit. *CsSWEET1* and *CsLOB1* were up-regulated in grapefruit following challenge with strain Xcc306Δ*pthA4::pthAw* (gray columns) in comparison with Xcc306Δ*pthA4* (black columns on left of gray columns). Quantitative RT-PCR was performed at 120 h after the inoculation. Data represent the mean ± SD.

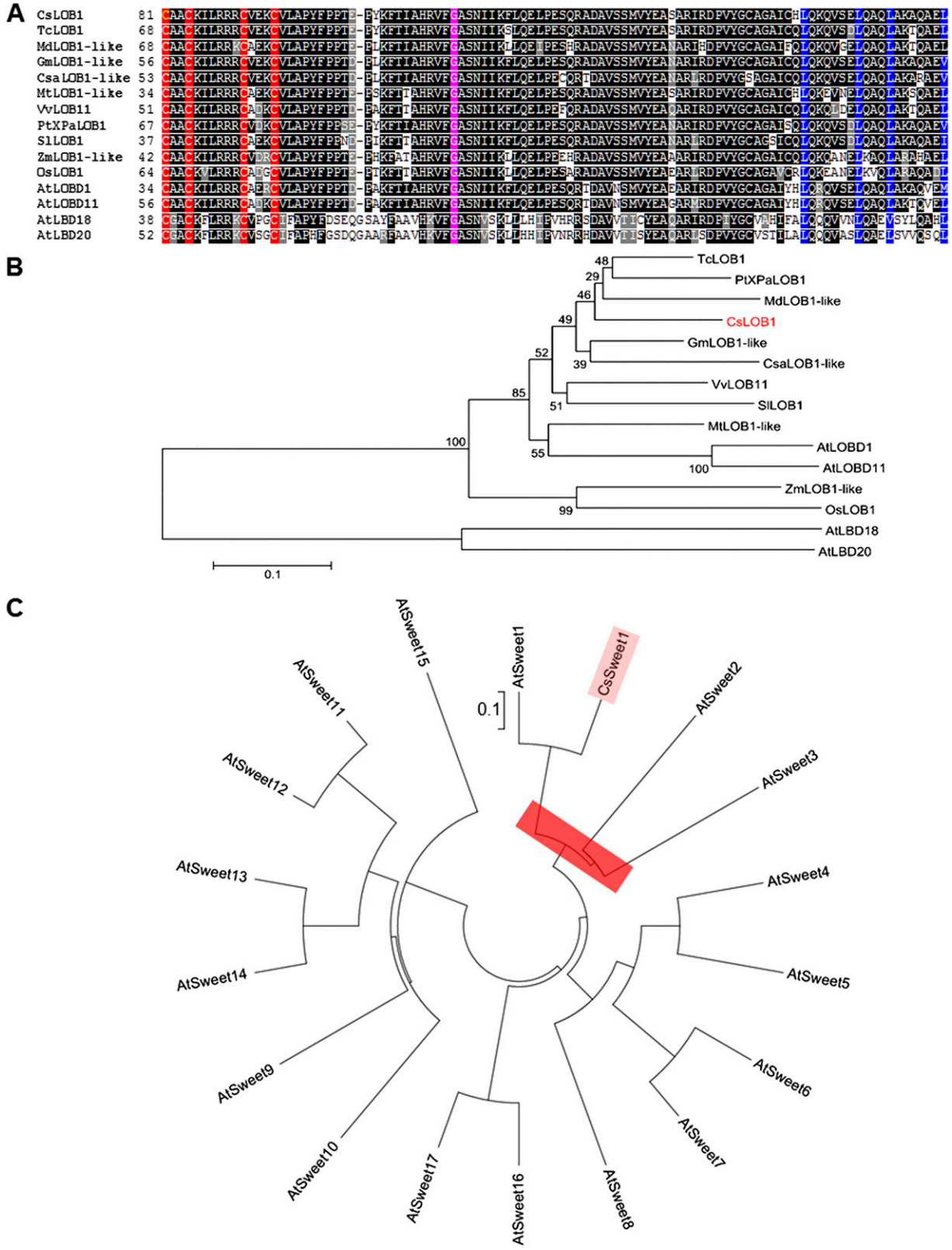

Fig. S4. Alignment and dendrogram of the Lateral Organ Boundaries (LOB) domain (LBD) family and SWEET family. (*A*) Alignment of select LOB family members from diverse plant species. *Citrus sinensis* (Cs), *Theobroma cacao* (Tc), *Malus domestica* (Md), *Glycine max* (Gm), *Cucumis sativus* (Csa), *Medicago truncatula* (Mt), *Vitis vinifera* (Vv), *Populus tremula* × *Populus alba* (PtXPa), *Solanum lycopersicum* (Solyc), *Zea mays* (Zm), *Oryza sativa* (Os), and *Arabidopsis thaliana* (At). Three conserved motifs, $CX_2CX_6CX_3C$, glycine residue, and $LX_6LX_3LX_6L$, are highlighted with red, pink, and blue, respectively. The alignment was conducted with CLUSTALW using default settings. (*B*) The phylogenetic tree was constructed using the neighbor-joining method with MEGA5.2 software. The numbers at the branches are bootstrap values for 1,000 repeats. The scale bar represents 0.1 substitutions per sequence position. (*C*) Phylogenetic tree of

Legend continued on following page

CsSWEET1 (highlighted) and the 17 closest SWEET family members from *Arabidopsis* (At). The phylogenetic tree was constructed (www.phylogeny.fr) of the closest amino acid sequences from *Arabidopsis* as obtained by a BlastP search of the Phytozome nonredundant protein database (www.phytozome.net). CsSWEET1 falls into the SWEET clade I, which includes *Arabidopsis SWEET1*, *2*, and *3* (*AtSweet1–3*).

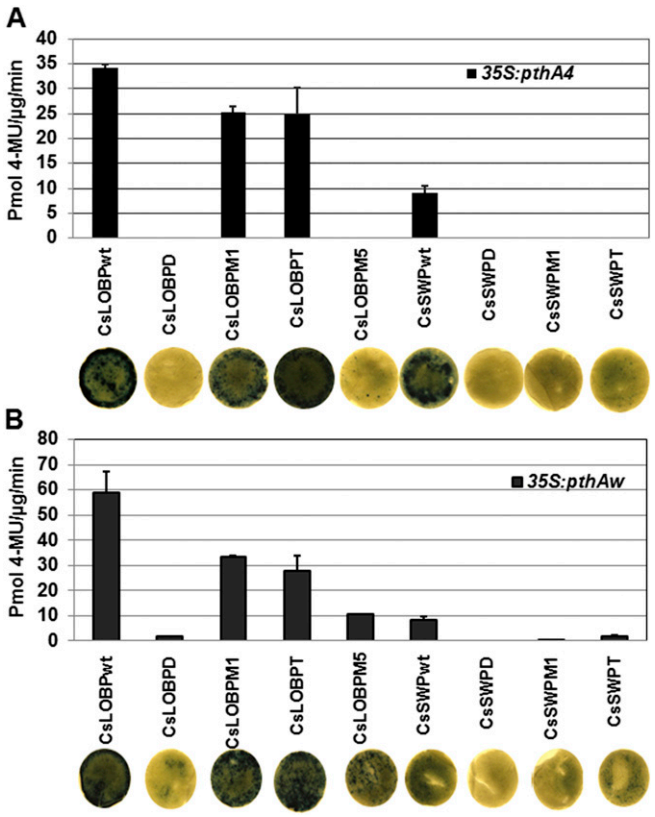

Fig. S5. PthA4 and PthAw drive the expression of *CsLOB1* and *CsSWEET1* promoters in *N. benthamiana*. Gene *pthA4* and *pthAw* coding sequences were cloned downstream of CaMV35S promoter in a binary T-DNA vector and transformed into *Agrobacterium LBA4404*, and codelivered with GUS reporter constructs as described in Fig. 4*A* into *N. benthamiana* leaf tissue. The GUS assays were conducted 3 d after the inoculation. Leaf discs were stained with X-Gluc (5-bromo-4-chloro-3-indolyl-b-D-glucuronide). Error bars indicate SD. (*A*) CaMv35S:*pthA4*. (*B*) CaMv35S:*pthAw*.

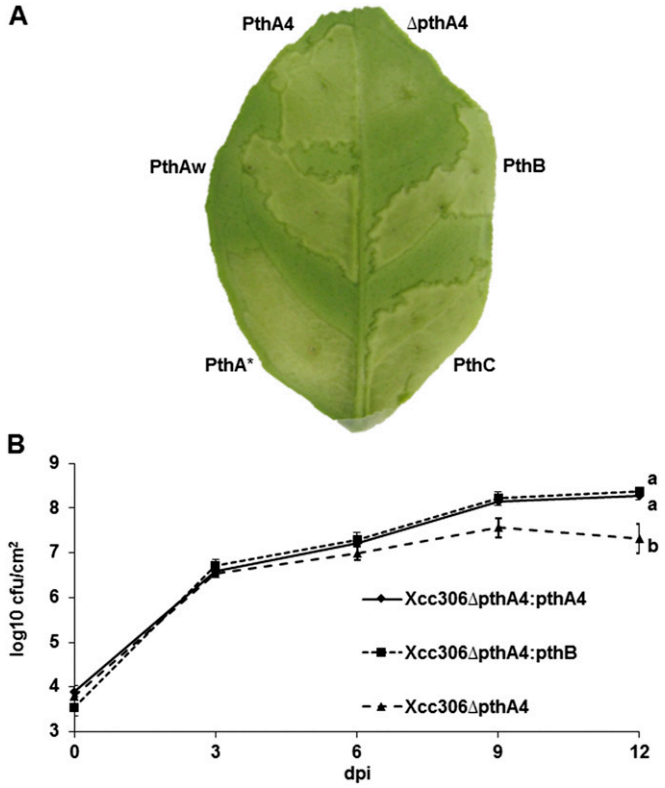

Fig. S6. PthA4 and homologs are critical for pustule formation and bacterial growth in leaf tissue. (*A*) The *pthA4* deletion mutant Xcc306Δ*pthA4* was complemented individually with TAL effectors PthA4, PthAw, PthA*, PthB, and PthC, respectively, and the resulting strains were inoculated on sweet orange. The inoculum concentration was 5×10^8 cfu/mL. The leaf was photographed 5 d after inoculation. (*B*) Strains Xcc306Δ*pthA4*::*pthB* and Xcc306Δ*pthA4*::*pthA4* have higher population than the mutant after 9 dpi. Sweet orange leaves were inoculated at the concentration of 5×10^5 cfu/mL, and the populations were measured at the time points indicated. Error bars represent 1 SD. The experiment was repeated twice with similar results. Values with the same letter (a or b) have no significant differences (at the $P \leq 0.01$ level) using ANOVA analysis and Tukey test.

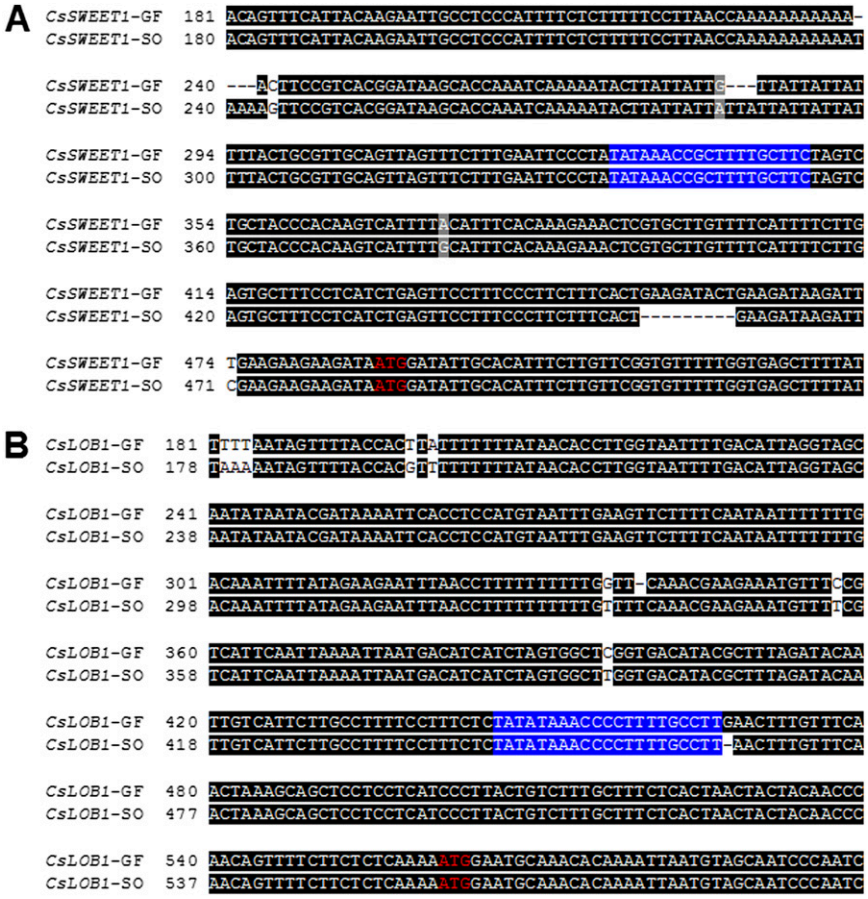

Fig. S7. Promoter sequences of *CsLOB1* and *CsSWEET1* in sweet orange (*A*) and grapefruit (*B*). GF, grapefruit; SO, sweet orange. Blue shading indicates predicated EBE_{PthA4}, and red indicates translation start site.

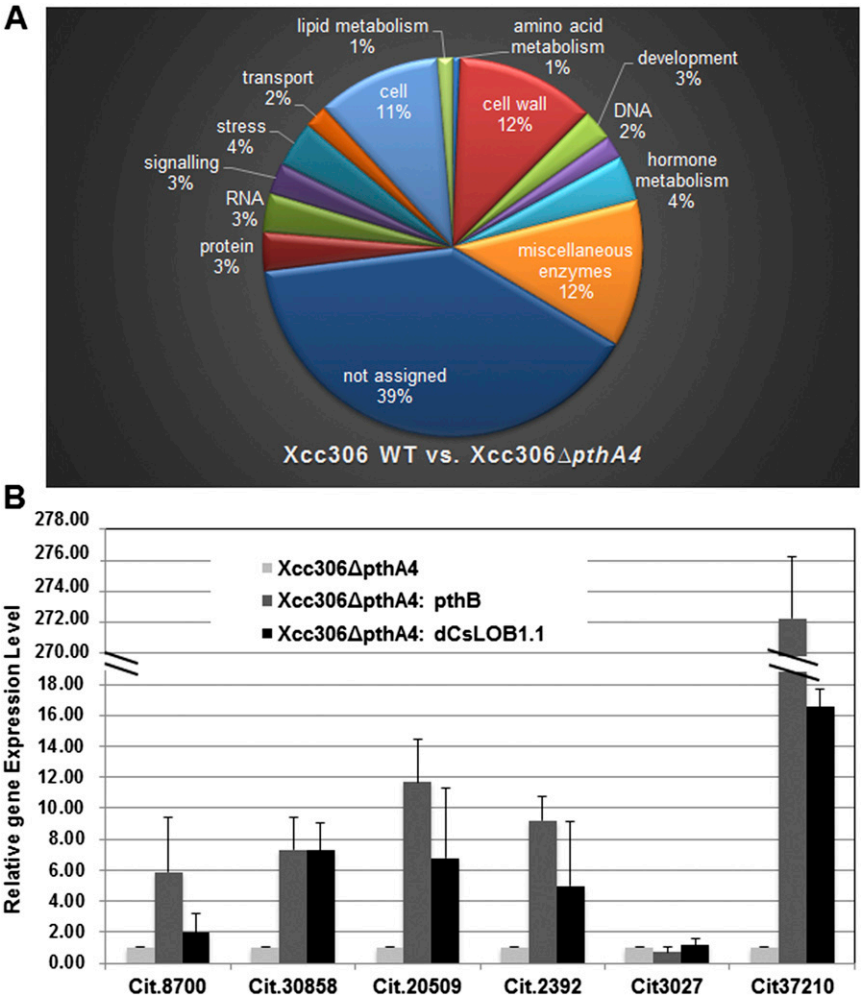

Fig. S8. Cell wall-related genes expression in sweet orange and grapefruit in association with natural and synthetic TAL effector-dependent expression of *CsLOB1*. (*A*) Functional category assignments of genes that induced in sweet orange by Xcc306 wild type relative to Xcc306Δ*pthA4*. Mercator analysis was performed using the genes in sweet orange with expression fold change more than 16 in Xcc306 vs. Xcc306Δ*pthA4* (108 elements) at 120 h after the infiltration. The functions were categorized using MapMan software. (*B*) Representative cell expansion or wall-related metabolism genes in grapefruit were activated by Xcc306Δ*pthA4::dCsLOB1.1* and Xcc306Δ*pthA4::pthB* when normalized to Xcc306Δ*pthA4*. Quantitative RT-PCR was conducted with gene-specific primers using samples of 120 h after the infiltration. The label probe identification numbers and annotations are listed as follows: Cit.8700, Cit.8700.1.S1_atextension; Cit.30858, Cit.30858.1.S1_at, expansin; Cit. 20509, Cit.20509.1.S1_at, pectate lyase; Cit. 2392, Cit.2392.1.S1_at, acidic cellulose; Cit. 3027, Cit.3027.1.S1_s_at*CsSWEET1*; Cit. 37210, Cit.37210.1.S1_at, lateral organ boundaries, *CsLOB1*.

Table S1. Strains and plasmids used in the study

Strain or plasmid	Relevant characteristics	Source
Strains		
Xanthonomans citri subsp. *citri*		
Xcc306	Group A, wild-type, Rif^r	DPI*
Xcc306Δ*pthA1*	*pthA1* deletion mutant	This study
Xcc306Δ*pthA2*	*pthA2* deletion mutant	This study
Xcc306Δ*pthA3*	*pthA3* deletion mutant	This study
Xcc306Δ*pthA4*	*pthA4* deletion mutant	This study
Xcc306Δ*pthA1*Δ*pthA2*Δ*pthA3*	*pthA1, pthA2, pthA3* deletion mutant	This study
Xcc306Δ*4pthA*	*pthA1 pthA2, pthA3, pthA4* deletion mutant	This study
Xcc306Δ*pthA4*:PthA4	PthA4 complement Xcc306Δ*pthA4*, Gm^r	This study
Xcc306Δ*pthA4*:Pthw	PthAw complement Xcc306Δ*pthA4*, Gm^r	This study
Xcc306Δ*pthA4*:PthA*	PthA* complement Xcc306Δ*pthA4*, Gm^r	This study
Xcc306Δ*pthA4*:PthB	PthB complement Xcc306Δ*pthA4*, Gm^r	This study
Xcc306Δ*pthA4*:PthC	PthC complement Xcc306Δ*pthA4*, Gm^r	This study
Xcc306Δ*pthA4*:*dCsLOB*	Artificial TALE targeting *CsLOB1* complement Xcc306*4pthA*Δ, Tc^r	This study
Xcc306Δ*pthA4*:*dCsSWEET*	Artificial TALE targeting *CsSWEET1* complement Xcc306Δ*pthA4*, Tc^r	This study
Escherichia coli		
DH5α	F$^-$*recA*ϕ80d*lac*ZΔM15	BRL†
DH5αλPIR	Host for pOK1; Sp^R, oriR6K, K2 replicon	(1)
Agrobacterium tumefaciens		
EHA105	Rif^r, Cm^r	
LBA4404	Contain pAL4404 plasmid	
Plasmid		
pOK1	Suicide vector, SacB	(1)
pRK2073	Sp^r Tra$^+$, helper plasmid	(2)
pBluescript KS(+)	Phagemid, pUC derivative, Amp^r	Stratagene
pLARF6	*rlx*$^+$RK2 replicon, Tc^r	(3)
pUFR053	repW, Mob$^+$, LacZα$^+$, Par$^+$, Gm^r	(4)
pBI101	Binary vector with *uidA* gene, Km^r	Clontech
pUC118/35S	pUC18 derivative with 35S, Amp^r	Gloria A. Moore (Horticultural Science Department, University of Florida)
pCAMBIA2200	Binary vector, Cm^r	Cambia

Amp, ampicillin; Cm, chloramphenicol; Gm, gentamicin; K_m, kanamycin; Sp, spectinomycin; Rif, rifamycin; Tc, tetracycline.
*DPI, Division of Plant Industry of the Florida Department of Agriculture and Consumer Services (Gainesville, FL).
†BRL, Bethesda Research Laboratories (Gaithersburg, MD).

1. Huguet E, Hahn K, Wengelnik K, Bonas U (1998) hpaA mutants of *Xanthomonas campestris* pv. *vesicatoria* are affected in pathogenicity but retain the ability to induce host-specific hypersensitive reaction. *Mol Microbiol* 29(6):1379–1390.
2. Daniels MJ, et al. (1984) Cloning of genes involved in pathogenicity of *Xanthomonas campestris* pv. *campestris* using the broad host range cosmid pLAFR1. *EMBO J* 3(13):3323–3328.
3. Staskawicz B, Dahlbeck D, Keen N, Napoli C (1987) Molecular characterization of cloned avirulence genes from race 0 and race 1 of *Pseudomonas syringae* pv. *glycinea*. *J Bacteriol* 169(12):5789–5794.
4. El Yacoubi B, Brunings AM, Yuan Q, Shankar S, Gabriel DW (2007) In planta horizontal transfer of a major pathogenicity effector gene. *Appl Environ Microbiol* 73(5):1612–1621.

Table S2. Primers used in this study

Primer	Sequence	Application
pthA1F	TGCCGCTTGCTGCAACAGAAG	Amplification of *pthA1* gene, including up- and downstream
pthA1R	TTGGCATCAGAGTGACGAACAC	
pthA2F	CGAGACCCTATACCGCGAG	Amplification of *pthA2* gene, including up- and downstream
pthA2R	CTGGACATACCAGACACTCCA	
pthA3F	GATCTGGCTGTCGGTAAAGCG	Amplification of *pthA3* gene, including up- and downstream
pthA3R	CCCTCACGCAAGCCGCTAT	
pthA4F	CACATAACGCGAGATTCCACG	Amplification of *pthA4* gene, including up- and downstream
pthA4R	TGCTTCAGTCCCTGATTGCC	
pthA4OEF	CCGCTCGAGCGGATGGATCCCATTCGTTCG	Amplification of *pthA4* gene for overexpression
pthA4OER	GGAAGATCTTCCCTGAGGCAATAGCTCCATCA	
37210F	TCCACCAACCGAACCATACA	Real-time PCR for *CsLOB1* gene
37210R	GGCACTTGCTTCATAGACCAT	
3027F	GTGAGCCTGAGAAACCATCG	Real-time PCR for *CsSWEET1* gene
3027R	CCGTTGCCGTTAGCCATCT	
EF1aF	GTAACCAAGTCTGCTGCCAAG	Real-time PCR for *CsEF1α* gene
EF1aR	GACCCAAACACCCAACACATT	
37210PF	CCCAAGCTTGGGAACCTTGACCTGGAATGG	Amplification of *CsLOB1* promoter
37210PR	CGCGGATCCGCGGCGTGGAGAAGATTGAGA	
3027PF	CCCAAGCTTGGGTTGACGGACACCTCTTAA	Amplification of *CsSWEET1* promoter
3027PR	CGGGATCCCGTAGCATTTCCTGGCAACA	
37210kpnF	GGGGTACCCCTTAACTTTGTTTCAACTAAAGC	Making EBE deleted *CsLOB1* promoter CsLOBPD
37210kpnR	GGGGTACCCCTATAGAGAAAGGAAAAGGC	
3027kpnF	GGGGTACCCCTTCTAGTCTGCTACCCACAA	Making EBE deleted *CsSWEET1* promoter CsSWPD
3027kpnR	GGGGTACCCCGGGAATTCAAAGAAACTAAC	
37210xhoF	CCGCTCGAGCCTTAACTTTGTTTCAAC	Making EBE mutated *CsLOB1* promoter CsLOBPM1
37210xhoR	CCGCTCGAGGGGTTTATATAGAGAAAG	
3027xhoF	CCGCTCGAGCTTCTAGTCTGCTACCCA	Making EBE mutated *CsSWEET1* promoter CsSWPM1
3027xhoR	CCGCTCGAGCGGTTTATATAGGGAATTC	
37210HindF	CCCAAGCTTGGGCTATATAAACCCCTTTTG	Making truncated *CsLOB1* promoter CsLOBPT
3027HindF	CCCAAGCTTCCTATATAAACCGCTTTTG	Making truncated *CsSWEET1* promoter CsSWPT
LOBPmut	CCCAAGCTTGGGCTATATAAACCtCTTTTGCCT	Making EBE mutated *CsLOB1* promoter CsLOBPM2
LOBPmug	CCCAAGCTTGGGCTATATAAACCggTTTTGCCT	Making EBE mutated *CsLOB1* promoter CsLOBPM3
LOBPig	CCCAAGCTTGGGCTATATAAACCCCTTgTTGCCT	Making EBE mutated *CsLOB1* promoter CsLOBPins
37210M5F	TTCTCGAGATAAACCCCTTTTGC	Making 5′ EBE mutated *CsLOB1* promoter CsLOBPM5
37210M5R	TACTCGAGAAAGGAAAAGGCAAG	
37210OEF	ACGCGTCGACATGGAATGCAAACACAAAAT	Amplification of *CsLOB1* gene for overexpression
37210OER	CCGCTCGAGATCATGTCCACAGAGGCTC	
3027OEF	CGCGTCGAC ATGGATATTGCACATTTCTTG	Amplification of *CsSWEET1* gene for overexpression
3027OER	CCGCTCGAGTCAAACTTGTTCAACTAGAGCC	
7877F	ACAGATTCAGCACAGAAGAGTT	Real-time PCR for Cit.7877.1.S1_at
7877R	GAAGCAAGGTCACCGTCAC	
2392F	CGTCAACCGTAAAAGCAGAA	Real-time PCR for Cit.2392.1.S1_at
2392R	GAGATGAACCCCTGTGATGAA	
5370F	CGTCCACAACAGCCAAAT12C	Real-time PCR for Cit.5370.1.S1_s_at
5370R	AGGCGTGCGATGAGAGATAC	
39387F	TGCTATTGGTGGAAGTGCTG	Real-time PCR for Cit.39387.1.S1_at
39387R	CACTCTCTGGTGCATCCTCA	